



Natural Resources
Canada

Ressources naturelles
Canada



Metamorphic contrast across the Kettle River fault, southeastern British Columbia, with implications for magnitude of fault displacement

J.F. Cubley and D.R.M. Pattison

Geological Survey of Canada

Current Research 2009-9

2009

Canada 

**Geological Survey of Canada
Current Research 2009-9**



**Metamorphic contrast across the Kettle River
fault, southeastern British Columbia, with
implications for magnitude of fault displacement**

J.F. Cubley and D.R.M. Pattison

2009

©Her Majesty the Queen in Right of Canada 2009

ISSN 1701-4387

Catalogue No. M44-2009/9E-PDF

ISBN 978-1-100-14265-4

A copy of this publication is also available for reference in depository libraries across Canada through access to the Depository Services Program's Web site at <http://dsp-psd.pwgsc.gc.ca>

A free digital download of this publication is available from GeoPub:
http://geopub.nrcan.gc.ca/index_e.php

Toll-free (Canada and U.S.A.): 1-888-252-4301

Recommended citation

Cubley, J.F. and Pattison, D.R.M., 2009. Metamorphic contrast across the Kettle River fault, south-eastern British Columbia, with implications for magnitude of fault displacement; Geological Survey of Canada, Current Research 2009–9, 19 p.

Critical reviewer

J. Ryan

Authors

J.F. Cubley

(jfcubley@ucalgary.ca)

D.R.M. Pattison

(pattison@ucalgary.ca)

Department of Geoscience

University of Calgary

2500 University Drive NW

Calgary, Alberta T2N 1N4

Correction date:

**All requests for permission to reproduce this work, in whole or in part, for purposes of commercial use, resale, or redistribution shall be addressed to: Earth Sciences Sector Copyright Information Officer, Room 644B, 615 Booth Street, Ottawa, Ontario K1A 0E9.
E-mail: ESSCopyright@NRCan.gc.ca**

Metamorphic contrast across the Kettle River fault, southeastern British Columbia, with implications for magnitude of fault displacement

J.F. Cubley and D.R.M. Pattison

Cubley, J.F. and Pattison, D.R.M., 2009. Metamorphic contrast across the Kettle River fault, southeastern British Columbia, with implications for magnitude of fault displacement; Geological Survey of Canada, Current Research 2009–9, 19 p.

Abstract: The Grand Forks metamorphic core complex (GFC) in southeastern British Columbia consists of North American–affinity metasedimentary rocks metamorphosed at upper amphibolite to granulite facies. The complex is separated from upper-greenschist to lower-amphibolite facies Quesnel Terrane lithologies by two north-south-trending Eocene normal faults: the Granby fault on the west and the Kettle River fault on the east. Estimates of metamorphic P-T conditions in the GFC and adjacent Quesnel Terrane rocks allow constraints on the metamorphic pressure contrast across the Kettle River fault. The peak metamorphic mineral assemblage in the basal paragneiss unit of the Grand Forks Complex (garnet+cordierite+sillimanite+K feldspar) is estimated at $750 \pm 20^\circ\text{C}$, 5.8 ± 0.6 kbar, and a low-pressure decompression metamorphic assemblage (spinel+cordierite) is constrained at $725 \pm 35^\circ\text{C}$, 3.2 ± 1.0 kbar. This high-temperature decompression occurred at least 9 Ma prior to movement the Kettle River fault and preserves evidence for a high-temperature, ~2.6 kbar exhumation event in the Late Cretaceous-early Paleocene. In the structural hanging wall, andalusite+cordierite-bearing siltstone in the contact aureole of the Jurassic Nelson granitoid suite was metamorphosed at $585 \pm 60^\circ\text{C}$, and 2.5 ± 0.5 kbar. The resulting metamorphic pressure contrast across the Kettle River fault is approximately 0.7 kbar (2.5 km), significantly less than that suggested by the large peak metamorphic contrast.

Résumé : Le complexe à noyau métamorphique de Grand Forks, dans le sud-est de la Colombie-Britannique, se compose de roches métasédimentaires aux affinités nord-américaines ayant été métamorphosées dans des conditions du faciès des amphibolites supérieur au faciès des granulites. Le complexe est séparé des lithologies du terrane de Quesnel, qui ont été métamorphosées dans des conditions du faciès des schistes verts supérieur au faciès des amphibolites inférieur, par deux failles normales de l'Éocène d'orientation nord-sud, soit la faille de Granby, à l'ouest, et la faille de Kettle River, à l'est. Les conditions de pression et de température métamorphiques dans le complexe de Grand Forks et les roches adjacentes du terrane de Quesnel permettent de délimiter le contraste de pression métamorphique de part et d'autre de la faille de Kettle River. Les paragenèses métamorphiques de l'unité basale de paragneiss du complexe de Grand Forks (grenat+cordiérite+sillimanite+feldspath potassique) rendent compte des conditions maximales de température et de pression du métamorphisme, qui sont estimées à $750 \pm 20^\circ\text{C}$ et à $5,8 \pm 0,6$ kbar, tandis qu'une paragenèse métamorphique témoignant d'une décompression à basse pression (spinel+cordiérite) circonscrit une température de $725 \pm 35^\circ\text{C}$ et une pression de $3,2 \pm 1,0$ kbar. Cette décompression à température élevée s'est produite au moins 9 millions d'années avant le déplacement à l'intérieur de la faille de Kettle River et les indices qui en ont été conservés témoignent d'un épisode d'exhumation d'environ 2,6 kbar à température élevée, au Crétacé tardif et au Paléocène précoce. Dans le toit de la faille, le siltstone à andalousite+cordiérite dans l'auréole de métamorphisme de contact de la suite granitoïde de Nelson du Jurassique a été métamorphisé à $585 \pm 60^\circ\text{C}$ et à $2,5 \pm 0,5$ kbar. Le contraste de pression métamorphique consécutif de part et d'autre de la faille de Kettle River s'élève à environ 0,7 kbar (2,5 km), ce qui est considérablement inférieur à ce que laissait croire l'important contraste dans les conditions maximales du métamorphisme.

INTRODUCTION

This study describes the metamorphic contrast across the Eocene Kettle River normal fault near Christina Lake, south-eastern British Columbia. The Kettle River fault forms the eastern boundary of the Grand Forks Complex (GFC), a metamorphic core complex comprising high-grade Proterozoic metasediments of North American affinity (Armstrong, 1988; Fyles, 1990; Acton et al., 2002; Höy and Jackaman, 2005), metamorphosed at upper-amphibolite to granulite facies. In the vicinity of Grand Forks, British Columbia, the complex is exposed in a narrow, approximately 15 km wide, fault-bounded window within low-grade metavolcanic and metasedimentary rocks of the Quesnel pericratonic terrane (Preto, 1970a; Erdmer et al., 1999; Unterschütz et al. 2002; Höy and Jackaman, 2005) (Fig. 1). South of the international border, in northeastern Washington State, the complex is known as the Kettle Dome (Cheney, 1980).

The Grand Forks Complex is one of a number of core complexes within the extensional Shuswap Complex of the Omineca Belt of southeastern British Columbia (Parrish et al., 1988). It was exhumed when the Omineca Belt, the tectonically thickened hinterland to the Cordilleran mountain belt, underwent a period of Eocene orogenic extension. The structurally lowest part of in the GFC, consisting predominantly of metasedimentary gneiss, has been tentatively correlated with the core gneiss complex of the Monashee Complex (also in British Columbia), exposed in the Thor-Odin and Frenchman Cap domes (Höy, 1987; Höy, 2001; Höy and Jackaman, 2005). This suggests a related depositional environment in the mid-Proterozoic. The subsequent tectonic history of the GFC is largely unknown, because unlike the Monashee and Valhalla complexes to the north, the GFC has not until recently (Laberge and Pattison, 2007) been investigated with regard to its metamorphic and geochronological history.

Our study in the vicinity of Christina Lake, southeastern British Columbia (Fig. 1, 2), attempts to characterize the metamorphism in the eastern portion of the GFC and adjacent low-grade Quesnel Terrane rocks, and thereby provide an estimate of the magnitude of displacement across the Kettle River fault. It complements the study of Laberge and Pattison (2007) on the Granby fault, which bounds the western side of the complex. Mineral-assemblage analysis is combined with thermodynamic modelling and mineral-chemical analysis to determine pressure-temperature conditions in the hanging wall and footwall to the Kettle River fault. Combined with existing geochronology, this allows an estimate of the pressure offset across the fault and provides new insight into the high-temperature exhumation history of the eastern GFC.

REGIONAL GEOLOGY

Grand Forks Complex

The GFC was first recognized by Brock (1903), who reported crystalline schist and gneiss between Christina Lake and Grand Forks, B.C. Daly (1912) noted that schist near Grand Forks was probably pre-Carboniferous, based on crosscutting relationships. Bowman (1950), working in northeastern Washington, recognized the continuation of the GFC into Washington (the Tenas Mary Creek sequence), assigning it a Precambrian age, and was the first to identify the Kettle River fault. The first comprehensive mapping of the complex in British Columbia was conducted by Little (1957), who included it in his 1:253 440 scale map of the east half of the Kettle River map area (NTS 082/E). It was mapped in more detail at a 1:50 000 scale by V. Preto for his Ph.D. thesis and subsequent Geological Survey of Canada volume (Preto, 1970a). All of this work was incorporated into an updated 1:250 000 compilation of the Pentiction (NTS 082/E) map area by Tempelman-Kluit (1989). More recent metamorphic and geochronological work by Laberge and Pattison (2007) focused on a small area on the western margin of the complex (Fig. 2), including the Granby fault.

The GFC comprises a varied succession of metasedimentary and closely associated igneous units (Preto, 1970a,b). The basal (structurally lowest) unit (unit I of Preto (1970a)) is a mixture of paragneiss, marble, calc-silicate and amphibolite gneiss, and has been correlated with the core paragneiss of the Monashee Complex by Höy and Jackaman (2005). Based on this correlation, the age of the metasedimentary basal unit was estimated at between approximately 1990 and 2000 Ma. However, a U-Pb detrital zircon age of 1681 ± 1.5 Ma and a composite Rb-Sr whole-rock age of 1695 ± 794 Ma from Armstrong et al. (1991), taken from a calcareous paragneiss of this unit, indicate a younger age of deposition.

A quartzite unit (unit II) unconformably overlies the basal unit and Höy and Jackaman (2005) tentatively correlated it with the middle-Proterozoic cover succession of the northern Monashee Complex. However, Preto (1970a) correlated this quartzite with the Cambrian Hamill Series in the Selkirk-Kootenay region, a unit in which coeval, syn-rift volcanic rocks have since been dated to a U-Pb zircon age of 596 ± 5.3 Ma by Colpron et al. (2002). This latter interpretation is supported by a U-Pb detrital zircon age of 650 ± 15 Ma for the GFC quartzite unit by Ross and Parrish (1991).

Above the quartzite is an upper Proterozoic to lower Paleozoic metasedimentary package (Units III, IV) similar to that found below the unconformity, comprising paragneiss, schist, calcsilicate, marble, and amphibolite. All of these units are intruded by Late Jurassic to Early Cretaceous granitoids (Höy and Jackaman, 2005). The core complex is metamorphosed to predominantly upper amphibolite facies, characterized by extensive migmatization in

paragneissic metasedimentary units. Local occurrences of granulite-facies mineral assemblages, characterized by hornblende+clinopyroxene+Opx in metabasite units, are found along the eastern margin of the complex. Whether the development of these assemblages represents higher temperature metamorphic conditions or different bulk rock compositions compared to other parts of the complex remains uncertain (Preto, 1970a; this study).

Hanging-wall lithologies

The hanging wall of the Kettle River fault is a complex mixture of metasedimentary rocks and intrusive rocks of various generations and compositions. In the Christina Lake area, the hanging-wall stratigraphy is dominated by the Mollie Creek assemblage and Elise Formation, both associated with the Quesnel Terrane, as well as the Jurassic Nelson and Eocene Coryell intrusive suites (Høy and Jackaman, 2005;

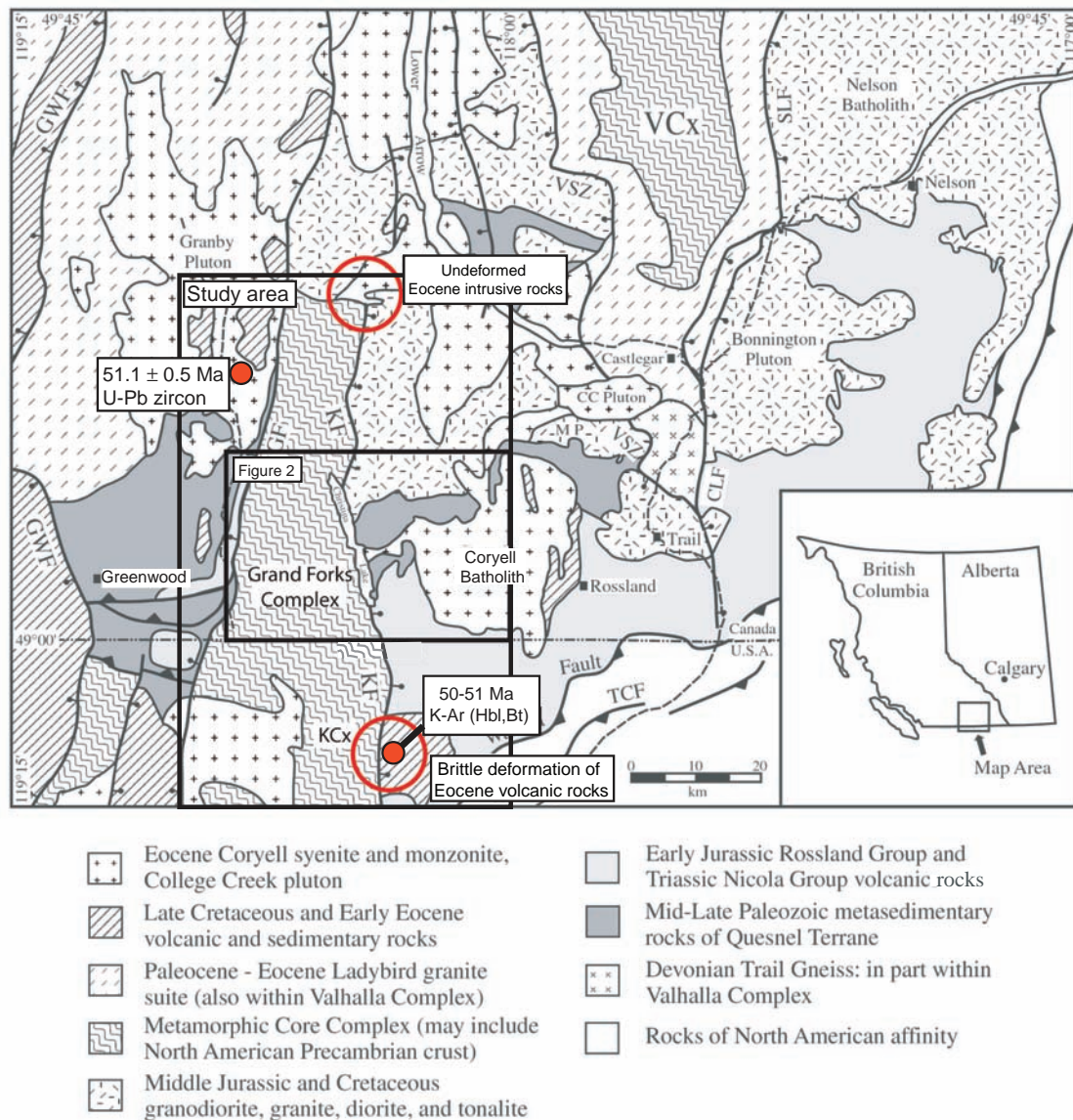


Figure 1. Simplified geology of the Omineca Belt in southern British Columbia and northeastern Washington. The Grand Forks Complex and study area is encompassed by the large rectangle, while the focused project area near Christina Lake, British Columbia (Fig. 2), is outlined by the inner rectangle. The two circles show key deformational relationships: the KRF does not cut Eocene Coryell Suite intrusive rocks north of Christina Lake (U-Pb zircon date from Carr and Parkinson (1989)), but does deform the Eocene Sanpoil Volcanics in northeast Washington (K-Ar overlapping hornblende-biotite age from Pearson and Obradovich (1977)). VCx = Valhalla Complex, KCx = Kettle Dome (Grand Forks Complex equivalent in NE Washington), GWF – Greenwood fault, KF – Kettle River fault, TCF – Tillicum Creek fault. Map adapted from Acton et al. (2002).

Acton et al., 2002). The Mollie Creek assemblage is composed of siltstone, calc-silicate, fine-grained schist, and marble of Pennsylvanian to Permian age, and has been tentatively correlated with the Mount Roberts Formation near Rossland by Acton et al. (2002). Tempelman-Kluit (1989) proposed an alternative correlation with the Ordovician-Devonian Lardeau Group in the Kootenay Terrane. Just north of the village of Christina Lake, the Mollie Creek assemblage is intimately interfingered with the late Triassic

(216 ± 1.4 Ma) Josh Creek diorite (Acton et al., 2002). The Elise Formation of the Rossland Group is predominantly comprised of metavolcanic and volcanoclastic rocks of early Jurassic age, with slivers of ultramafic rocks exposed by west-verging thrust faults (Höy and Jackaman, 2005). In the Rossland area, the Elise Formation unconformably overlies the Mount Roberts Formation, and if one accepts the correlation of Acton et al. (2002) and Höy and Dunne (1997), it is

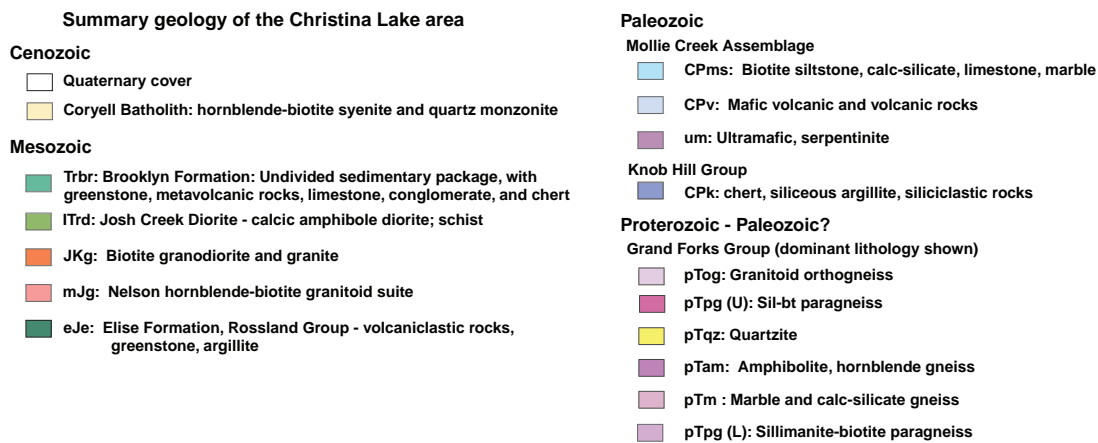
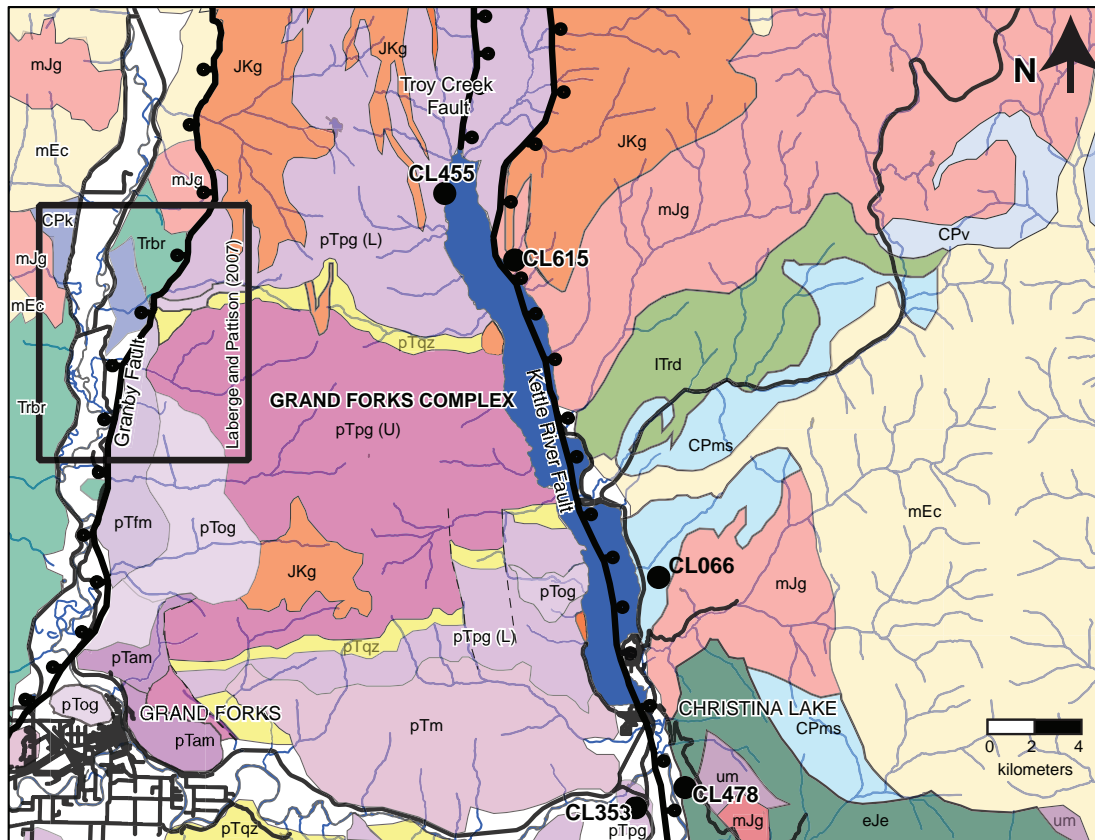


Figure 2. Simplified geology of the Grand Forks Complex and associated hanging-wall lithologies in the vicinity of Grand Forks and Christina Lake, British Columbia. The study area of Laberge and Pattison (2007) is shown, as are the sampling locations for the two samples used to quantify the pressure contrast across the Kettle River fault (CL066 and CL455), and samples used to characterize deformation style (CL353, CL478, and CL615). Map adapted from Höy and Jackaman (2005).

likely that the same stratigraphic relationships apply in the Christina Lake area, although contacts between the two units have not been observed.

The Mollie Creek assemblage, Josh Creek diorite, and Elise Formation predate the intrusion of granitoids of the Middle Jurassic Nelson Suite and syenites and monzonites of the Eocene Coryell Batholith. The emplacement of the Nelson Suite created a contact aureole characterized by cordierite±andalusite-bearing, low-pressure mineral assemblages in metasilstone about 1.5 km from the pluton contact, and migmatized K-feldspar+cordierite±andalusite siltstones approximately 300 m from the contact in the Sutherland Creek area east of Christina Lake. The Eocene Coryell Batholith (51.1 ± 0.5 Ma; Carr and Parkinson, 1989) appears to have intruded at a lower temperature or shallower structural level than the Nelson Suite, as contact metamorphic effects are limited, generally to within 20 m of the intrusive contact.

Kettle River fault

The Kettle River fault is a north-trending, east-dipping normal fault that extends for 40 km north of the border in British Columbia and for 45 km south of the border in Washington State (Rhodes and Cheney, 1981). The fault has not been observed in outcrop in British Columbia, but it was described by Rhodes and Cheney (1981) near Barstow, Washington, where it is exposed in the floor of the Kettle River Valley. In British Columbia it is covered by surficial deposits or by Christina Lake, but bordering outcrops are abundant enough to tightly constrain its position north of the lake, and to characterize the nature of deformation in both the hanging wall and footwall. In the footwall, a shallowly dipping mylonitic fabric is crosscut by regular, spaced chlorite and epidote veins up to about 1 km west of the fault trace, with increasing sericitization and alteration nearer the fault (site CL353, Fig. 2, 3a,b, and 4b). In addition, coarse-grained leucosomes and granitic injections in the gneisses have undergone varying degrees of cataclasis.

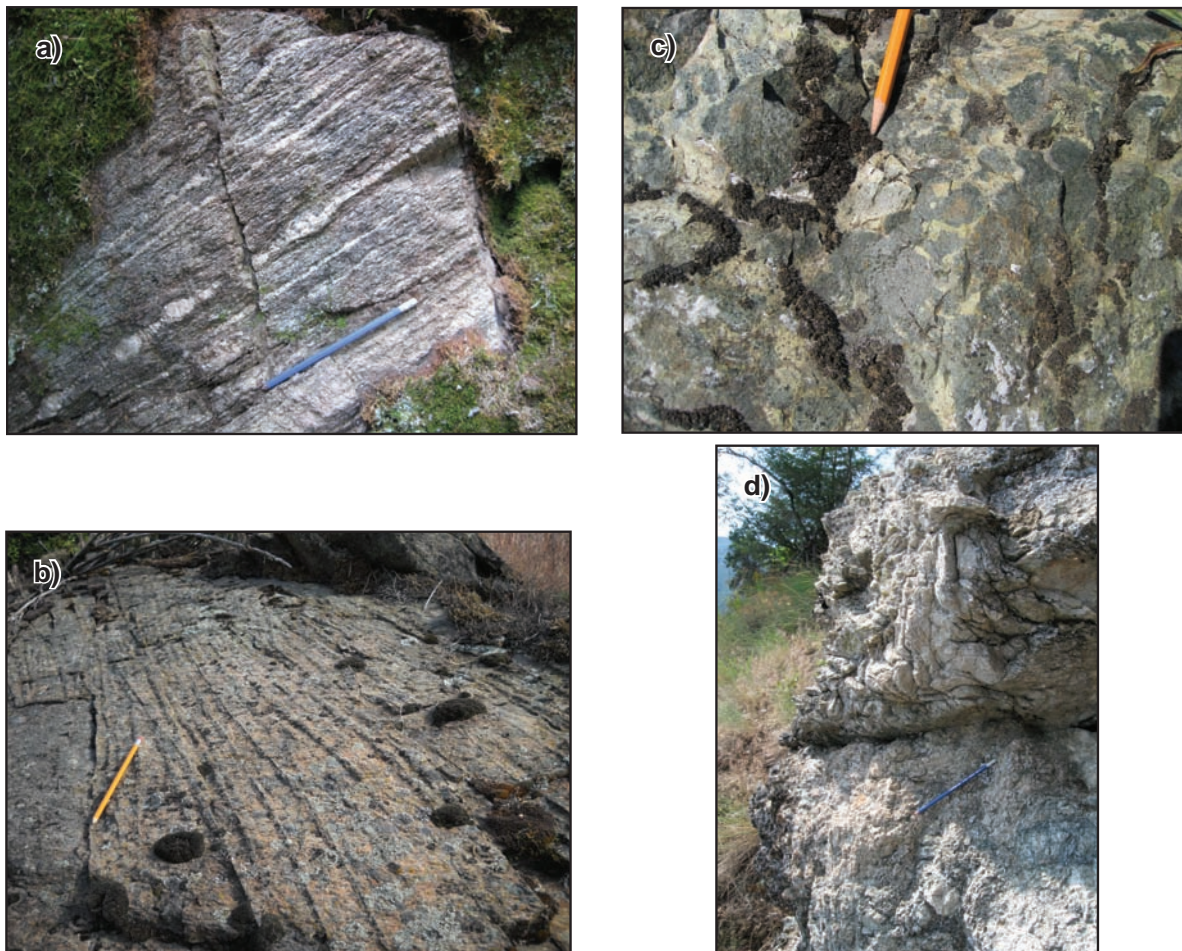


Figure 3. Field photographs of deformation textures related to the Kettle River normal fault (KRF). **a)** Ductile mylonitic fabric in footwall orthogneiss at site CL353. 2009-384. **b)** Spaced chlorite-epidote veins in GFC paragneiss, weathering resistant due to associated silicification halos (site CL353). 2009-382. **c)** Brecciated Elise Formation volcanic rock, with epidote surrounding remnant volcanic fragments (site CL478). 2009-392. **d)** Cataclastic Nelson Suite granite (site CL615). 2009-381.

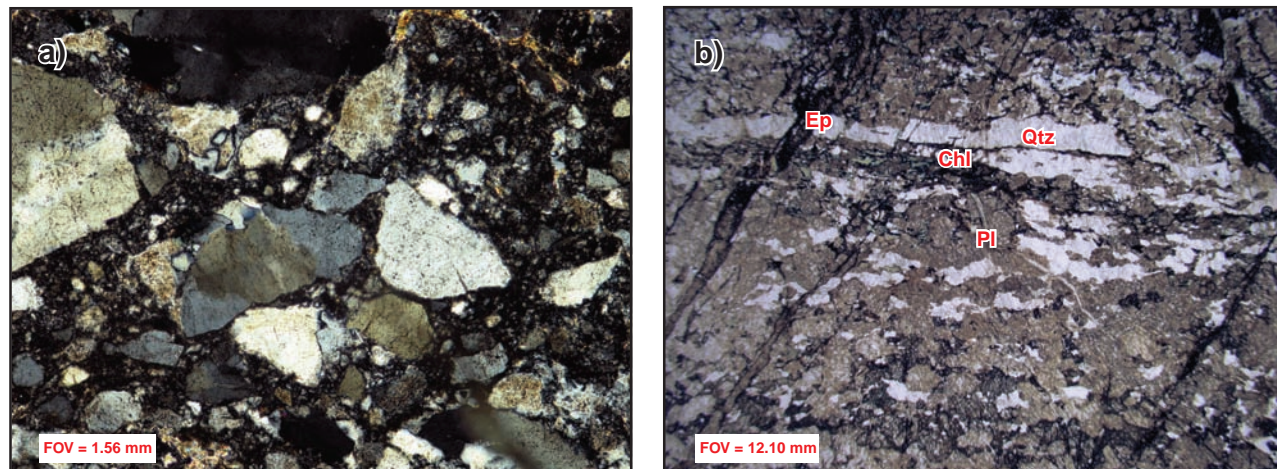


Figure 4. Photomicrographs of deformation textures related to the Kettle River fault. **a)** Brittle cataclasite from the hanging-wall granitic rock of the Nelson Suite (CL615). 2009-387. Note grain size reduction and remnant angular feldspar fragments. **b)** Brittle overprint on a mylonitized footwall granodiorite (CL353) with elongated quartz ribbons. Parallel epidote+chlorite veins crosscut the mylonitic fabric, and plagioclase is highly sericitized (2009-391). FOV – field of view.

The hanging wall to the KRF appears to have experienced a greater degree of brittle deformation than the footwall (site CL615, Fig. 2, 3d, and 4a), with cataclastic deformation and grain-size reduction observed up to 300 m east of the fault trace in Nelson Suite granitoids at the north end of Christina Lake. Closest to the fault zone, spaced fracture sets dip shallowly to the east (presumed parallel to dip on the KRF), and between these shallowly dipping sets are finely spaced, steeply dipping fracture sets. The latter fracture sets have abundant slickenlines — however, the scatter of slickenline orientations precludes determination of a consistent vector of slip. Slickenlines are not found on the shallowly dipping fracture sets. In the southern part of the field area, the Elise Formation volcanoclastic rocks are heavily fragmented, with remnant clasts isolated by intense chlorite, calcite, and epidote alteration for at least 500 m from the presumed fault trace (site 478, Fig. 2 and 3c).

The timing of movement along the KRF is constrained to be 51–50 Ma by two relationships (Fig. 1). South of the border in northeastern Washington, near the hamlet of Orient, Eocene lava, volcanic breccia, and tuff of the Sanpoil Volcanics exhibit brittle deformation attributed to the KRF (Cheney, 1980; Rhodes and Cheney, 1981). The Sanpoil Volcanics were dated at 51–50 Ma (K-Ar, hornblende and biotite) by Pearson and Obradovich (1977). North of Christina Lake, the fault is truncated by the undeformed Eocene Coryell Batholith (Tempelman-Kluit, 1989; Fig. 1). While the exact age is unknown at this location, Carr and Parkinson (1989) dated Coryell-Suite intrusive rocks (the Granby Pluton) on the western side of the complex at 51.1 ± 0.5 Ma (U-Pb, zircon) (Fig. 1).

NATURE, DISTRIBUTION, AND MINERALOGY OF METAMORPHIC ROCKS

A suite of samples from the footwall and hanging wall of the Kettle River fault was petrographically examined to characterize metamorphic mineral assemblages, shown in Figure 5. This map also includes petrography results presented in Laberge and Pattison (2007) for the Volcanic Creek area on the western margin of the Grand Forks Complex. A transect across the core complex within the structurally low-est paragneiss unit was completed to check for changes in the peak metamorphic mineral assemblage across the complex. In the hanging wall, the fine grain size and intimate textural relationships of many metamorphic minerals (e.g. intergrowths of hornblende and actinolite in meta-andesite) precluded accurate identification of those minerals in the field, so sample localities observed in thin section are shown in Figure 5. The main metamorphic assemblages observed in hanging wall and footwall lithologies are described in the following sections, with reference to localities in Figure 5.

Petrography of rocks in the footwall of the KRF

Pelitic rocks

Aluminous paragneisses, interpreted to represent highly metamorphosed pelites, constitute the bulk of the Grand Forks Complex in the Christina Lake area. The most common mineral assemblage is sillimanite+biotite+K feldspar+plagioclase+quartz+ilmenite paragneiss, with greatly varying abundances of garnet, cordierite, and spinel. Apatite,

tourmaline, zircon, and monazite are common accessory phases. Within the basal paragneiss unit, there is no apparent variation in this pelitic mineral assemblage across the complex (Fig. 5). All paragneissic rocks throughout the complex are migmatitic, interpreted to reflect partial melting accompanying high-grade metamorphism. A postmetamorphic

mylonitic fabric with a strong, shallowly plunging, east-southeast sillimanite lineation is observed in most samples along the eastern margin of the complex.

Cordierite is predominantly found as a replacement mineral in coronas around garnet and mesosome sillimanite, but also occurs in the matrix. The degree to which cordierite has

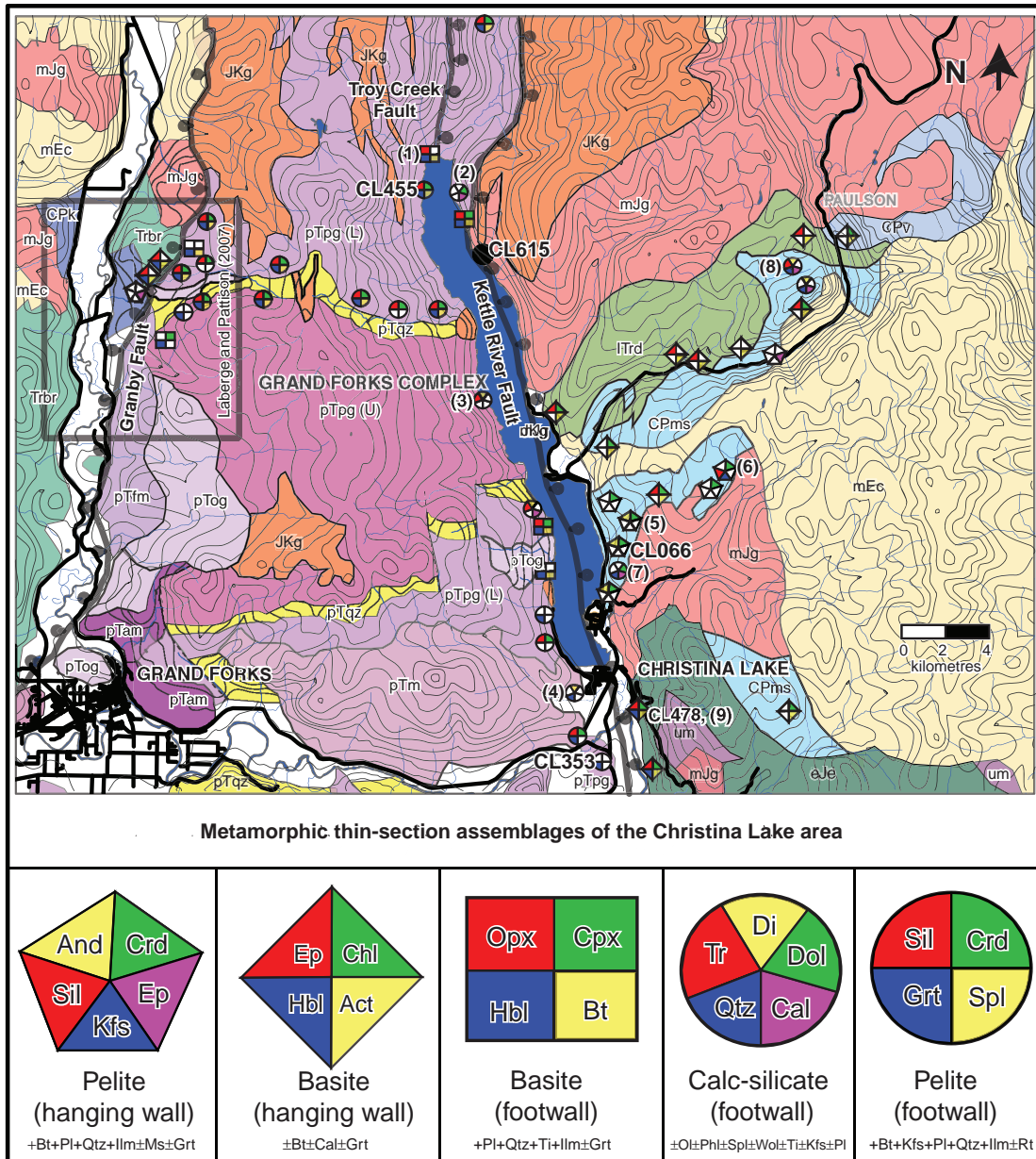


Figure 5. Metamorphic mineral assemblages observed in thin section for the hanging wall and footwall of the Kettle River fault. Assemblages along the Granby fault are taken from Laberge and Pattison (2007). Numbers (e.g. (4)) identify locality locations referred to in the petrographic description section, whereas sample locations used in characterizing fault deformation and metamorphic grade are referred to by their site name (e.g. CL353). See text and tables for further details. Unit colours and abbreviations as in Figure 2. Act – actinolite, And – andalusite, Bt – biotite, Cal – calcite, Chl – chlorite, Cpx – clinopyroxene, Crd – cordierite, Di – diopside, Dol – dolomite, Ep – epidote, Grt – garnet, Hbl – hornblende, Ilm – ilmenite, Kfs – K feldspar, Ms – muscovite, Ol – olivine, Opx – orthopyroxene, Phl – phlogopite, Pl – plagioclase, Qtz – quartz, Rt – rutile, Sil – sillimanite, Spl – spinel, Ti – titanite, Tr – Tremolite, Wol – wollastonite.

replaced garnet and sillimanite varies considerably between samples. Spinel is observed in mesosomes where there has been reaction of sillimanite to cordierite, and to a lesser degree in cordierite coronas surrounding garnet. Ilmenite is highly concentrated within altered sillimanite+cordierite mesosome bands. Any muscovite observed appears to be retrograde. Sillimanite-free, garnet+biotite gneisses occur interleaved within Al paragneisses, and the protolith of these gneisses is difficult to resolve. However, due to their common association with aluminous metasedimentary gneisses, they have been assigned a sedimentary origin in Figure 5.

Basic rocks

Amphibolitic rocks across the southern Grand Forks Complex were characterized geochemically by Preto (1970b) and interpreted to have an igneous origin, regardless of whether they were found spatially associated with the metasedimentary rocks, or as sills within the metasedimentary succession. On the eastern margin of the complex, the scattered metabasite rock is dominated by a hornblende+biotite+plagioclase+quartz mineral assemblage with localized occurrences of clinopyroxene, orthopyroxene, and garnet. Titanite and apatite are locally abundant as accessory phases. Biotite is consistently subordinate to hornblende, and quartz is widespread but rare. Garnet was observed only in one outcrop at the north end of Christina Lake (locality 1, Fig. 5), being as large as 3 to 4 cm, and is highly poikilitic.

Amphibolite, like the paragneiss, is generally well foliated and crosscut by granitic leucosome, most likely generated in the surrounding migmatitic paragneiss. Elongation lineations defined by hornblende appear to parallel those defined by sillimanite, plunging shallowly toward the east-southeast. The metamorphic mineral assemblages indicate upper amphibolite facies in most parts of the complex, however, occurrences of granulite-facies mineral assemblages (characterized by orthopyroxene+clinopyroxene-bearing assemblages), are scattered along the shores of Christina Lake (Fig. 5). No granulite-facies, orthopyroxene+clinopyroxene-bearing amphibolites were reported along the Granby fault by Laberge and Pattison (2007), but this may be a function of the restricted field area of that study, inappropriate bulk compositions, or post-granulite-facies retrogression along the fault.

Calc-silicate and marble rocks

Only four calcsilicate samples from the footwall of the Kettle River fault were studied with the petrographic microscope, and their mineralogy and textures vary considerably. Calc-silicate rocks are typically closely interfingered with paragneisses within pelitic map units. Near the north end of Christina Lake, a phlogopite+spinel+olivine+calcite+dolomite+rutile coarse-grained marble is massive and unfoliated despite its proximity to the KRF, (locality 2, Fig. 4). Phlogopite and olivine are large and abundant, while spinel is

observed in trace amounts. On the western side of the lake are abundant calc-silicate outcrops, composed of diopside+tremolite+wollastonite+K feldspar+plagioclase+titanite±epidote (locality 3, Figure 5). Coarse-grained tremolite forms splays within virtually monomineralic bands, and is also found as smaller inclusions within diopside. Potassium feldspar is abundant, predominantly within diopside-bearing horizons, and titanite is found only in trace amounts. Calcite-rich marble is found in outcrop-scale horizons interlayered with the tremolite+diopside calc-silicate, but calcite does not appear to be part of the calc-silicate mineral assemblage. In various hand samples, garnet is contained within tremolite-diopside layers. While there are distinct compositional horizons, the outcrops on the western edge of the lake are typically weakly foliated to unfoliated. Well foliated, diopside-bearing, calc-silicate gneisses, characterized by the assemblage diopside+plagioclase+titanite+epidote+quartz±K feldspar, with late calcite and chlorite and accessory apatite, occur at the southern end of Christina Lake (locality 4, Fig. 5). Differences in metamorphic assemblages in the calc-silicate rocks across the area are attributed to differences in bulk rock-composition rather than metamorphic grade.

Petrography of rocks in the hanging wall of the KRF

Pelitic and semipelitic rocks

Pelitic to semipelitic siltstone in the hanging wall of the Kettle River fault makes up a large part of the Pennsylvanian-Permian Mollie Creek assemblage, and displays a range of textures and mineral assemblages. Compositionally layered siltstone, best observed in roadcuts along Highway 3 northeast of Christina Lake, most commonly contains an assemblage of biotite+plagioclase+epidote+quartz+muscovite, with accessory pyrite and ilmenite. Greenish-yellow, lighter-coloured layers are rich in epidote and muscovite, and purplish-brown darker bands contain biotite and accessory pyrite and ilmenite, with plagioclase and quartz found in both horizons. Near Christina Lake, compositional layering within siltstones is less distinct to non-existent. Rock fabrics range from unfoliated and hornfelsic to schistose, depending on the size and abundance of phyllosilicate phases, and proximity to intrusive bodies.

Just east of Christina Lake, siltstone near the contact with the middle Jurassic Nelson plutonic suite displays a variety of contact-metamorphic textures and mineral assemblages, the most common assemblage of which is biotite+cordierite+plagioclase+quartz+ilmenite±andalusite±muscovite (locality 5, Fig. 5). Cordierite forms large porphyroblasts that are wrapped by a late foliation, yet preserve an older, unfoliated fabric within, represented by unoriented biotite inclusions. Andalusite is less common and, where present, less abundant than cordierite, and is typically restricted to thin zones between adjacent cordierite porphyroblasts. Farther east in the Sutherland Creek drainage, metasiltstone

contains a cordierite+K feldspar+plagioclase+quartz+ilmenite± sillimanite±andalusite assemblage, with abundant migmatitic textures and partial to complete pinitization of cordierite (locality 6, Fig. 5). Migmatization extends for at least 200 m from the pluton contact. Muscovite typically partially pseudomorphs sillimanite knots and appears to be out of textural equilibrium with the peak assemblage. Sillimanite and andalusite have not been observed in the same thin section. Within this zone of migmatization occur non-migmatitic, cordierite-bearing siltstone devoid of potassium feldspar, muscovite, or an aluminosilicate phase. This lack of migmatization may be attributed to a less aluminous or potassic bulk composition that is unsuitable for melt production at this metamorphic grade.

Carbonate rocks

Samples from the Fife marble quarries just east of Christina Lake display calcite+dolomite+quartz+talc assemblages, and are mainly unfoliated (locality 7, Fig. 5). Talc is found along the contact between quartz and carbonate segregations as small fans and 'booklets' and trace epidote is present in veins. Rare calcite+tremolite±garnet skarns are observed as thin, <5 m wide bands (Acton, 1998; this study). In the Burnt Basin area near Paulson, northeast of Christina Lake, carbonate rocks near the contact with the Jurassic Nelson granitoid suite are intensely ductilely deformed (locality 8, Fig. 5). Carbonate samples observed in the Burnt Basin area have tremolite+calcite+quartz±diopside±epidote±dolomite assemblages, and host significant sphalerite, galena, and pyrrhotite mineralization in carbonate-replacement/skarn-type showings (L. Caron, unpub. rpt., 2003; this study). Carbonate has deformed plastically around diopside crystals suggesting that ductile deformation occurred syn- to post-contact metamorphism, while temperatures were still elevated. Massive-sulphide mineralization appears to postdate ductile fabric development, as aligned tremolite crystals define inclusion trails within sphalerite. Skarn outcrops within these ductilely deformed carbonates contain the assemblage garnet+calcite+epidote and are found as discrete layers ≤25 m thick that lack the strong fabric exhibited in the surrounding rock. Small outcrops of similar ductilely deformed limestone occur near the contact between the Nelson Suite and Mollie Creek assemblage just east of Christina Lake, though they grade abruptly into the unfoliated Fife marbles (locality 7, Fig. 5).

Basic rocks

Metabasite rocks in the hanging wall can be grouped into two main categories: the intrusive Triassic Josh Creek diorite, and volcanic and volcanoclastic rocks within the Rossland Group and Mollie Creek assemblage. In the Josh Creek diorite body northeast of Christina Lake, microdiorite was variably deformed and subjected to regional greenschist-facies metamorphism. Highly foliated microdiorite locally is

compositional layered on the thin-section scale, with deformed hornblende+plagioclase and clinopyroxene+plagioclase segregations and epidote+garnet veins. Microdiorite samples have an original igneous assemblage of clinopyroxene+plagioclase+quartz+biotite±hornblende with accessory zircon and titanite, and later metamorphism resulted in the addition of metamorphic actinolite+chlorite+epidote. In many samples actinolite occurs as pseudomorphs after clinopyroxene, whereas epidote and chlorite are predominantly concentrated as small crystals in the rock matrix. Some samples show well developed coronas of chlorite replacing clinopyroxene.

Metavolcanic rocks are found in the Permian-Pennsylvanian Mollie Creek assemblage near Paulson and in the Lower Jurassic Rossland Group southeast of Christina Lake. The original igneous assemblage in the Rossland Group volcanic rocks appears to have been clinopyroxene+biotite+plagioclase+quartz+titanite±hornblende, identical to that found in the Josh Creek diorite, but finer grained. Chlorite, epidote, and actinolite are the predominant minerals in the metamorphic assemblage, with actinolite replacing clinopyroxene phenocrysts and biotite commonly altered to chlorite. All three metamorphic minerals occur in the rock matrix. Microprobe-element mapping of two Rossland Group volcanic samples show intergrowths of hornblende and actinolite replacing clinopyroxene, suggestive of transitional greenschist-amphibolite-facies metamorphism (locality 9, Fig. 5), like that described on the west side of the GFC by Laberge and Pattison (2007). It is possible that similar transitional hornblende+actinolite intergrowths occur in other localities in the volcanic rocks and the Josh Creek diorite intrusions, as proposed in Acton (1998). However, as this is speculative, volcanic and dioritic samples that have not yet been analyzed using the electron microprobe are shown in the assemblage map in Figure 5 as being hornblende-free.

The mineral assemblages in the three hanging-wall lithologies (pelite, carbonate, and basite rocks), indicate that a greenschist- to transitional amphibolite-facies regional assemblage predominates in samples distal to contacts with the Nelson granitoid suite. Near those contacts, peak metamorphic assemblages reflect contact metamorphism, with grade increasing to upper amphibolite facies as indicated by K feldspar+melt zone assemblages.

PETROGRAPHY AND MINERAL COMPOSITIONS OF SAMPLES USED FOR PRESSURE-TEMPERATURE ESTIMATION

Estimates of pressure-temperature conditions in the hanging wall and footwall were obtained from a suite of metapelitic samples from the immediate hanging wall and footwall to the KRF. The petrography and petrology of one representative sample from the hanging wall and footwall are discussed in detail below. These samples contain mineral

assemblages and equilibrium textures characteristic of multiple samples from the metamorphic units, lack extensive late, low-temperature alteration (e.g. chloritization of biotite), and are comparatively fine grained and homogeneous, yielding bulk rock XRF analyses that best represent the effective bulk compositions available during metamorphic mineral growth.

Petrography of footwall sample CL455

Sample CL455 was taken from the basal Proterozoic paragneiss unit (unit I in Preto (1970a)) of the GFC, on the western edge of Christina Lake (Fig. 2). The sample is a migmatitic paragneiss with the mineral assemblage sillimanite+garnet+cordierite+biotite+K feldspar+plagioclase+quartz+ilmenite+spinel, that is weakly mylonitized with a top-

to-the-east sense of shear. Minor amounts of the accessory phases apatite, monazite, zircon, and rutile are also present. Sillimanite, garnet, and biotite are found in thin mesosomes typically 1 to 2 mm wide, and quartz and K feldspar are concentrated in coarser leucosomes, 1 to 12 mm wide. Quartz, plagioclase, and K feldspar make up approximately 65% of the modal mineralogy of the rock, in the approximate ratio of 5:3:1. Plagioclase feldspar is within both mesosome and leucosome layers as small subhedral to anhedral grains (~0.2–0.8 mm). Sillimanite (5%) is medium to coarse grained, in the form of elongate prismatic to acicular needles that are rimmed by heavily pinitized cordierite, ilmenite and spinel (Fig. 6a). Dark-green spinel grains are anhedral, small (<0.1mm), and enclosed in cordierite. Ilmenite up to 0.8 mm in size is also found in matrix mesosome and as inclusions in garnet. Biotite constitutes about 20% of the modal mineralogy and is concentrated in the mesosome, but is also found

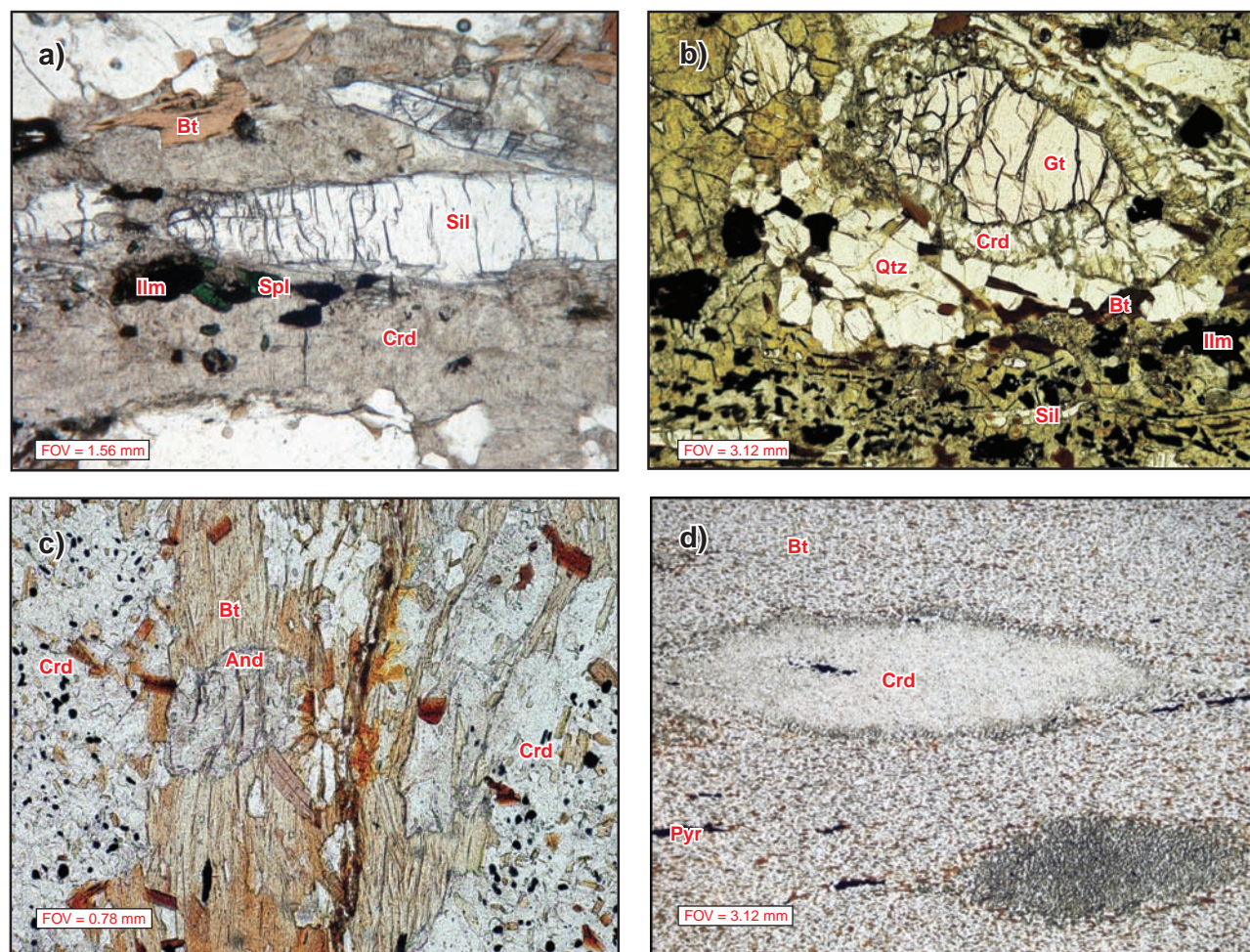


Figure 6. Photomicrographs of footwall (a, b) and hanging-wall (c, d) samples near the Kettle River fault. **a)** Highly pinitized cordierite with associated ilmenite and spinel rimming elongate prismatic sillimanite (CL455). 2009-388. **b)** Corona of cordierite and quartz around garnet, and ilmenite and cordierite replacing sillimanite in altered mesosome (CL455). 2009-380. **c)** Anhedral andalusite porphyroblast postdating foliated cordierite porphyroblasts (CL066). 2009-383. **d)** Elongate cordierite porphyroblasts oriented within a foliation defined by small oriented biotite lathes and pyrrhotite mineralization (CL066). 2009-385). FOV = field of view. Mineral abbreviations as in Figure 5.

in leucosomes and in distinct concentrations along the mesosome-leucosome boundary. Subhedral biotite lathes have a consistently larger grain size in mesosomes (0.4–1.3 mm) than in leucosomes (up to 0.5 mm). Garnets (5–7% modal mineralogy) are 0.6 to 1.4 mm in size, subhedral to anhedral, and are rimmed by partially pinitized cordierite and quartz, with cordierite forming an innermost corona and quartz exterior of cordierite (Fig. 6b). In addition to forming reaction rims around garnet and sillimanite, cordierite is also found in the matrix as small anhedral grains of varying size that are completely altered to pinite.

Element mapping of garnets within CL455 was conducted using the electron microprobe at the University of Calgary. Overall, compositional zoning was minimal, with the exception of thin reaction rims with Ca^{2+} and Mg^{2+} depletion and Fe^{2+} and Mn^{2+} enrichment (Fig. 7). Quantitative analyses were conducted on garnet, cordierite, plagioclase, biotite and spinel, with an accelerating voltage of 15kV and a beam current of 10 nA. A beam diameter of 5 μm was maintained for all minerals, and all analyses were subjected

to matrix corrections based on the ZAF method (e.g. Reed, 1996). Representative mineral analyses for sample CL455 are given in Table 1.

The Mg number ($\text{Mg}/(\text{Mg}+\text{Fe})$) in garnet cores averaged 0.26 (0.25–0.26), while matrix biotite compositions averaged Mg# 0.46 (0.44–0.48). Garnet compositions were measured in the cores of grains, as the lower $\text{Mg}/(\text{Mg}+\text{Fe})$ ratio and Mn enrichment in the rim suggested re-equilibration with the matrix at a lower temperature than peak metamorphism. In reaction rims around garnet and sillimanite, cordierite has an average Mg# of 0.48 (0.47–0.48), while spinel has an average Mg# of 0.08 (0.07–0.11). Spinel has a variable gahnite component, with $\text{Zn}/(\text{Zn}+\text{Fe}^{2+}+\text{Mg}+\text{Mn})$ ratios ranging from 0.026–0.039. As the microprobe cannot measure $\text{Fe}^{2+}/\text{Fe}^{3+}$ ratios, Fe^{3+} was calculated in garnet and spinel using the formulation of Droop (1987), $F = 2X(1-T/S)$, where F is the number of Fe^{3+} ions, X is the number of oxygens in the mineral formula, T is the ideal number of cations per formula unit, and S is the observed cation total per X oxygens when all iron is assumed to be Fe^{2+} . Matrix plagioclase compositions averaged An_{21} with a range from An_{19} – An_{24} .

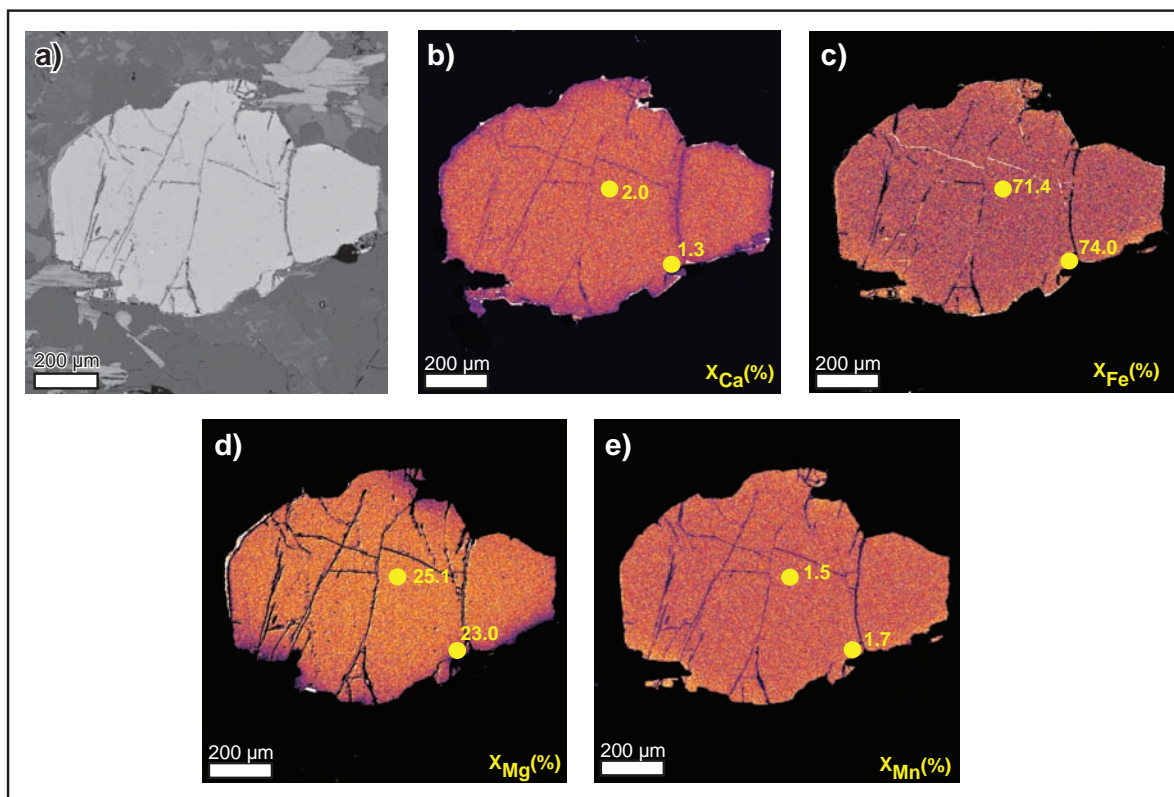


Figure 7. Electron microprobe composition maps for a garnet from CL455 sillimanite+garnet+biotite+cordierite paragneiss, including: **a)** back-scatter image. 2009–390. **b)** Homogeneity in x_{Ca} weight percent (%) through the core of the garnet, with depletion in a thin-reaction rim. 2009–379. **c)** homogeneity in x_{Fe} weight percent. 2009–389. **d)** Homogeneity in x_{Mg} weight percent. 2009–393. **e)** Mn weight percent. 2009–386. Notice Ca and Mg depletion in the garnet rims, and associated enrichment in Mn and Fe. Brighter colours indicate higher concentrations of the element of interest. Growth zoning is absent. $X_{\text{Ca}}(\%) = \text{Ca}/(\text{Ca}+\text{Mg}+\text{Fe}+\text{Mn})$; $X_{\text{Fe}}(\%) = \text{Fe}/(\text{Fe}+\text{Mn}+\text{Mg}+\text{Ca})$; $X_{\text{Mg}}(\%) = \text{Mg}/(\text{Mg}+\text{Fe}+\text{Mn}+\text{Ca})$; $X_{\text{Mn}}(\%) = \text{Mn}/(\text{Mn}+\text{Mg}+\text{Fe}+\text{Ca})$. Mineral abbreviations as in Figure 5.

Table 1 a) Bulk XRF major-element and ICP-MS trace-element geochemistry for samples CL066 (hanging wall) and CL455 (footwall). **b)** Mineral chemistry from electron microprobe analyses on sample CL455.

a)			b)						
Sample	CL066	CL 455	Rock: sillimanite-garnet-cordierite-biotite paragneiss (CL455)						
Rock	Crd-And-Bt siltstone	Sil-Gt-Bt-Crd paragneiss	Mineral:	Garnet	Garnet	Cordierite	Plagioclase	Biotite	Spinel
Oxide	wt%/ppm		Note:	core	rim	rxn rim	matrix	matrix	rxn rim
SiO ₂	61.62	67.81	Oxide	Wt%					
TiO ₂	1.120	0.627	SiO ₂	38.026	37.879	46.820	62.898	35.403	0.000
Al ₂ O ₃	16.66	15.61	Al ₂ O ₃	21.393	21.098	32.983	24.026	17.649	51.231
Fe ₂ O ₃	9.41	5.07	Fe ₂ O ₃	0.655	0.650	--	--	--	7.293
MnO	0.140	0.064	FeO	32.512	33.499	11.594	0.184	18.665	33.820
MgO	2.61	1.03	MnO	0.683	0.769	0.195	0.000	0.037	0.159
CaO	1.83	1.01	MgO	6.406	5.847	6.120	0.000	8.738	1.623
Na ₂ O	1.45	4.55	Na ₂ O	--	--	0.182	8.184	0.198	--
K ₂ O	3.54	3.16	K ₂ O	--	--	0.002	0.290	8.962	--
P ₂ O ₅	0.128	0.057	CaO	0.697	0.471	0.002	4.497	0.000	--
BaO	1151	756	Cr ₂ O ₃	0.000	0.000	0.000	--	--	1.247
Ce	31	88	ZnO	--	--	--	--	--	4.339
Co	17	-2	TiO ₂	0.040	0.000	--	--	5.888	0.011
Cr ₂ O ₃	111	93	Total	100.412	100.213	97.898	100.079	95.540	99.723
Cu	99	48	Cations						
Ni	32	10	Si	2.988	2.997	4.925	2.775	5.299	0.000
Sc	22	18	Al ³⁺	1.981	1.967	4.089	1.249	3.113	1.807
V	244	60	Fe ³⁺	0.039	0.039	0.000	0.000	0.000	0.164
Zn	79	0	Fe ²⁺	2.136	2.216	1.020	0.007	2.336	0.847
LOI	1.57	0.67	Mn ²⁺	0.045	0.052	0.017	0.000	0.005	0.004
Total	100.26	99.77	Mg ²⁺	0.750	0.689	0.960	0.000	1.950	0.072
Ga	19.0	18.6	Na ⁺	0.000	0.000	0.037	0.700	0.057	0.000
Nb	4.8	12.9	K ⁺	0.000	0.000	0.000	0.016	1.711	0.000
Pb	1.9	21.4	Ca ²⁺	0.058	0.040	0.000	0.213	0.000	0.000
Rb	58.0	94.9	Cr ³⁺	0.000	--	--	--	--	0.030
Sr	167.6	186.1	Zn ²⁺	0.000	--	0.000	0.000	0.000	0.096
Th	4.5	15.2	Ti ⁴⁺	0.002	0.000	0.000	0.000	0.663	0.000
U	1.1	2.3	Sum	8.000	8.000	11.049	4.959	15.134	3.021
Y	22.9	35.3	M/FM	0.256	0.234	0.485	--	0.455	0.067
Zr	130.2	244.1	xMn (Grt)	0.015	0.017	xAb	0.754		
S (wt%)	0.40	0.07	xCa (Grt)	0.020	0.013	xAn	0.229		
						xOr	0.018		

Major elements are in wt%, trace elements are in ppm.
Crd- cordierite, And-Andalusite,
Bt- biotite, sil-sillimanite, Gt-garnet

Fe₂O₃ is calculated using formula of Droop (1987)
Number of cations is based on structural formulae with 18, 12, 22, 8, and 4 oxygens for cordierite, garnet, biotite, plagioclase, and spinel, respectively.
M/FM = Mg/(Mg+Fe);
X_{Mn} = Mn/(Mn+Mg+Ca+Fe²⁺); X_{Ca} = Ca/(Ca+Fe²⁺+Mg+Mn); X_{Ab} = Na/(Na+K+Ca);
X_{An} = Ca/(Ca+Na+K); X_{Or} = K/(K+Ca+Na).

Petrography of footwall sample CL066

Sample CL066 is a metasiltstone with metamorphic mineral assemblage of biotite+cordierite+andalusite+plagioclase+quartz+ilmenite+muscovite, collected from the Mollie Creek assemblage in the hanging wall of the Kettle River fault. It lies within the poorly defined contact aureole of the Nelson granitoid suite, approximately 800 m from the contact. Biotite (40%) defines the fabric of the rock and forms subhedral lathes up to 0.15 mm. Equigranular, fine-grained plagioclase and quartz with grain sizes of 0.025 to 0.075mm form approximately 30% of the modal mineralogy with 5% ilmenite scattered throughout the matrix. Poikilitic cordierite porphyroblasts (25–30%) are up to 3.2 mm in length and oriented within a strong foliation that wraps the porphyroblasts (Fig. 6d). Unoriented biotite grains are preserved as inclusions in the centre of the porphyroblasts, but an outer rim of cordierite growth contains a distinct foliation with

strongly oriented biotite grains. This is suggestive of at least two stages of cordierite growth. Andalusite (<1%) is found in the interface between closely adjacent cordierite porphyroblasts (Fig. 6c). It includes fine oriented biotite lathes and quartz grains parallel to the matrix foliation. Andalusite is fine-grained (up to 0.2 mm), and anhedral. Muscovite is found only in trace amounts.

PRESSURE TEMPERATURE DETERMINATION AND PHASE DIAGRAM MODELING

Bulk chemical XRF analyses for major elements were obtained for the Christina Lake area samples described above, using a Philips PW2440 4kW automated spectrometer system at McGill University. Trace elements were analyzed

by ICP-MS. All analyses are shown in Table 1. Isochemical phase-diagram sections for these bulk compositions were constructed in the $\text{MnO}_2\text{-Na}_2\text{O-CaO-K}_2\text{O-FeO-MgO-Al}_2\text{O}_3\text{-SiO}_2\text{-H}_2\text{O-TiO}_2$ (MnNCKFMASHT) system using the Gibbs free-energy minimization software THERIAK-DOMINO (de Capitani and Brown, 1987; de Capitani, 1994) and the Holland and Powell (1998) thermodynamic database, updated to incorporate the solution models in Tinkham and Ghent (2005). The phase-diagram sections for samples CL066 and CL455 are shown in Figures 8 and 9a, respectively. In CL066, the s Table assemblage formed under subsolidus conditions, and therefore the sample was modelled with excess water in the system. The migmatitic paragneiss, sample CL455, was metamorphosed above the solidus and consequently a melt model (White et al., 2007) was incorporated in the modelling. Two main assumptions in this melt modelling are: 1) all water available for melting was contained in the hydrous phases s Table on the wet solidus, and 2) the rock was closed to the loss of melt and therefore to the loss of H_2O (Spear et al., 1999; Holtz and Johannes, 1994). Whole-rock water content in sample CL455 was estimated from that contained in the predicted modal amounts of muscovite and biotite at 5.8 kbar, 635°C, approximately 1°C below the wet solidus at the 5.8 kbar pressure estimate of Laberge and Pattison (2007) for the peak metamorphic assemblage in paragneiss on the western edge of the complex at 84 ± 3 Ma. Below the wet solidus, the system was treated as water saturated. Fractional effects were ignored, consistent with relatively rapid elemental diffusion in high-grade metamorphism.

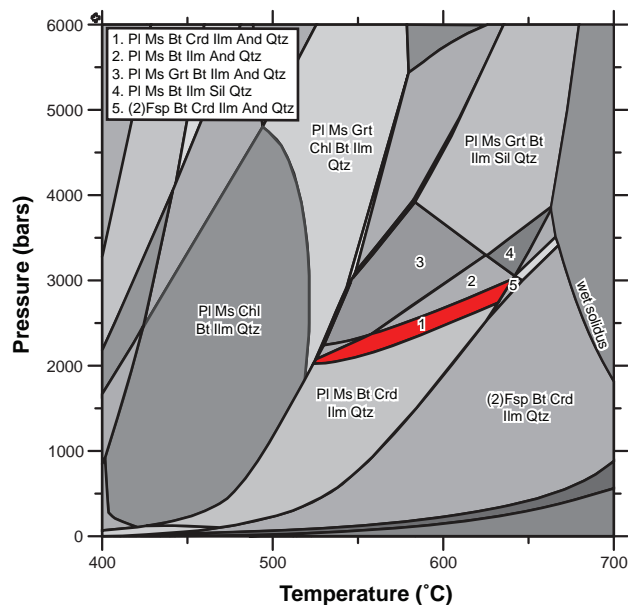


Figure 8. MnNCKFMASHT ($\text{MnO-Na}_2\text{O-CaO-K}_2\text{O-FeO-MgO-Al}_2\text{O}_3\text{-SiO}_2\text{-H}_2\text{O-TiO}_2$) isochemical phase diagram for hanging-wall andalusite+cordierite metasilstone. Mineral abbreviations as in Figure 5.

Hanging Wall

In Figure 8, the cordierite-andalusite stability field in sample CL066 provides an effective pressure constraint (but a poorer temperature constraint) of $585 \pm 60^\circ\text{C}$, 2.5 ± 0.5 kbar for metamorphic conditions in the contact aureole of the Jurassic Nelson Suite. The lack of evidence for a regional metamorphic overprint suggests that the hanging wall was not subsequently buried to significantly greater depths. This estimate overlaps with the peak metamorphic pressure estimate for the hanging wall to the Granby fault on the western edge of the complex, 2.3 ± 0.7 kbar, (Laberge and Pattison, 2007), although the timing of that metamorphism was unconstrained.

Footwall

The isochemical phase diagram for sample CL455 is shown in Figure 9a. Of note is a thin, low-variance stability field of biotite+sillimanite+cordierite+garnet+K feldspar that separates the garnet+sillimanite+biotite and garnet+cordierite+biotite stability fields between 660°C , 3.4 kbar and 770°C , 6.5 kbar. The presence of the complete low-variance assemblage in sample CL455 suggests that the sample falls within or near this stability band, recognizing that multivariance from minor elements may widen the interval represented by the modelled mineral assemblage. In order to better constrain the P-T conditions, mineral composition isopleths were calculated using Theriak-Domino for the Mg# ($\text{Mg}/(\text{Fe}+\text{Mg})$ ratio) in garnet and biotite (Fig. 9b,c), and X_{Mn} ($\text{Mn}/(\text{Mn}+\text{Fe}+\text{Mg}+\text{Ca})$) and X_{Ca} ($\text{Ca}/(\text{Ca}+\text{Mg}+\text{Fe}+\text{Mn})$) in garnet (Fig. 9d,e). Isopleths for Mg# of cordierite were also calculated (Fig. 9f). Measured mineral compositions were then plotted on these isopleth maps as red bands showing the range of results, with a dashed line indicative of the average.

Figure 10 summarizes the results and compares them with P-T estimates of Laberge and Pattison (2007) from the western side of the Grand Forks Complex, the latter based on thermobarometry in conjunction with petrogenetic grid constraints. The lack of coincidence between the biotite and garnet isopleths temperatures in this study (Fig. 9b,c), in particular the Fe-rich biotite compositions, may be accounted for by the retrograde net transfer reaction $\text{garnet} + \text{K-feldspar} + \text{H}_2\text{O} = \text{sillimanite} + \text{biotite} + \text{plagioclase}$, proposed by Spear and Parrish (1996) for high-grade gneisses of the same mineralogy from the nearby Valhalla Complex. Observations by Robinson (1991) and Spear and Florence (1992) showed that garnet core compositions combined with partially retrograded matrix biotite can yield erroneous temperature estimates in excess of 100°C above the metamorphic peak if subjected to retrograde net transfer reactions like the one above. The possibility of this reaction in sample CL455 is supported by the garnet element maps (Fig. 7), which show a thin rim of iron enrichment, and garnet-biotite thermometry,

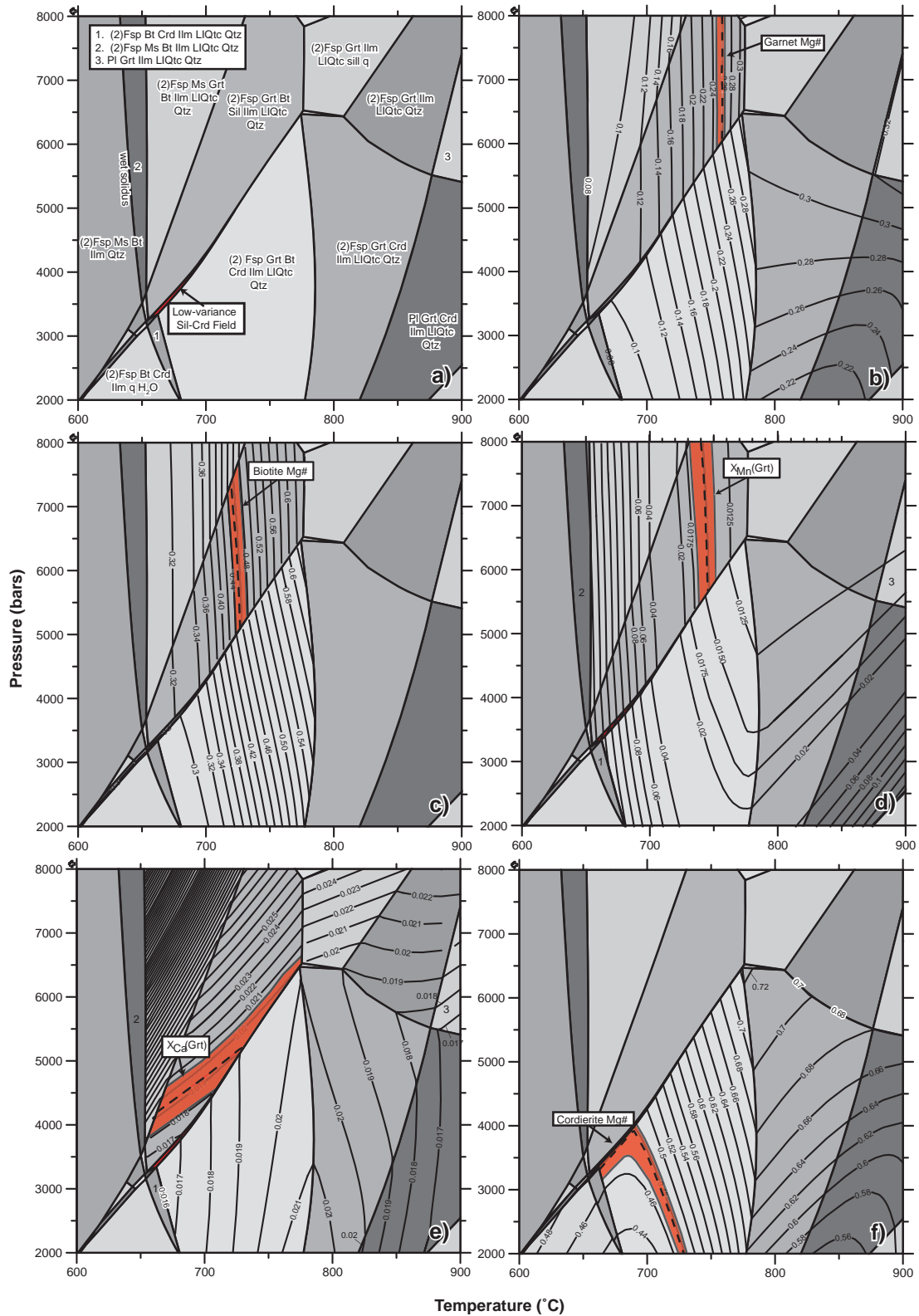


Figure 9. a) Phase diagram for sillimanite+garnet+biotite+cordierite+K feldspar paragneiss, GFC. Note low-variance sillimanite+cordierite stability field which contains sample CL455. b) Mg# mineral composition isopleths for garnet (avg. = 0.257) in sample CL455, with red band illustrating values obtained from microprobe analysis of the minerals, and average microprobe values shown by dashed lines. c) Biotite Mg# isopleths (avg. = 0.455). d) X_{Mn} isopleths for garnet (avg. = 0.015). e) X_{Ca} isopleths for garnet (avg. = 0.019). f) Mg# isopleths for cordierite from the decompression assemblage (avg. = 0.478). Mineral abbreviations as in Figure 5.

which yields anomalously high temperature estimate of approximately 1060°C at 6.0 kbar, using the calibration and program of Dasgupta et al. (2004).

Based on the above considerations, we propose that the isopleths from garnet core compositions better represent peak temperature conditions. These intersect at $750 \pm 20^\circ\text{C}$, 5.8 ± 0.6 kbar (Fig. 10), consistent with the requirement that the peak P-T must lie within or close to the narrow low-variance biotite+sillimanite+garnet+cordierite+K feldspar stability field. The pressure estimate of this study is indistinguishable from the pressure estimate of Laberge and Pattison (2007); however the corresponding temperature estimate is approximately 50°C lower, although within the combined error of the two estimates.

Concerning the cordierite-spinel corona assemblage, Laberge and Pattison (2007) proposed the following reaction in KFMASH for its development: *garnet+sillimanite+melt = cordierite + spinel + quartz + K feldspar*. In the full ten-component MnNCKFMASHT system this reaction probably also involves plagioclase and ilmenite. However, a spinel-cordierite assemblage does not appear on the phase diagram section in Figure 9a, suggesting that the decompression reaction that produced the coronas may not have involved the entire bulk composition but only aluminum-rich, silica-poor compositional domains (e.g. Johnson et al., 2004). Therefore the corona cordierite isopleths in Figure 9f, and the resultant P-T estimate of $700 \pm 35^\circ\text{C}$, 3.0 ± 1.0 kbar from them, are of uncertain significance. Better constraints may come from two stability fields for cordierite+spinel-bearing assemblages from other studies: one from a petrogenetic grid in KFMASH ($\text{K}_2\text{O-FeO-MgO-}$

$\text{Al}_2\text{O}_3\text{-SiO}_2\text{-H}_2\text{O}$) for high-grade pelites from the western GFC constructed by Laberge and Pattison (2007), and the second from a MnNCKFMASHT ($\text{MnO-Na}_2\text{O-CaO-K}_2\text{O-FeO-MgO-Al}_2\text{O}_3\text{-SiO}_2\text{-H}_2\text{O-TiO}_2$) phase diagram section for Al-rich compositional domains around garnet and sillimanite by Johnson et al. (2004). These two stability fields overlap, and the temperature of their overlap (725°C) was used for geobarometry calculations using cordierite-spinel relationships in the $\text{FeO-Al}_2\text{O}_3\text{-SiO}_2\text{-ZnO}$ (FASZn) system (Nichols et al., 1992). Results suggest a pressure of 3.2 ± 1.0 kbar at 725°C , which falls within the stability fields presented in those two studies (Fig. 10). Based on the above results, P-T conditions accompanying spinel-cordierite corona development are therefore estimated to be $725 \pm 35^\circ\text{C}$, 3.2 ± 1.0 kbar, with a maximum temperature constraint of 770°C given the assumption that there was not additional heating past the peak P-T temperature ($750 \pm 20^\circ\text{C}$). The above estimate is lower than, but within error of, the $800 \pm 90^\circ\text{C}$, 4.2 ± 0.8 kbar estimate for similar assemblages in the western part of the GFC by Laberge and Pattison (2007).

DISCUSSION

High-temperature decompression in the Grand Forks Complex, based upon the above P-T results, was on the order of 2.6 kbar (9.2 km), assuming a uniform crustal density of 2.85 g/cm^3 (Spear, 1993). The lack of a significant temperature drop accompanying this decompression (Fig. 11) is consistent with a rapid exhumation event.

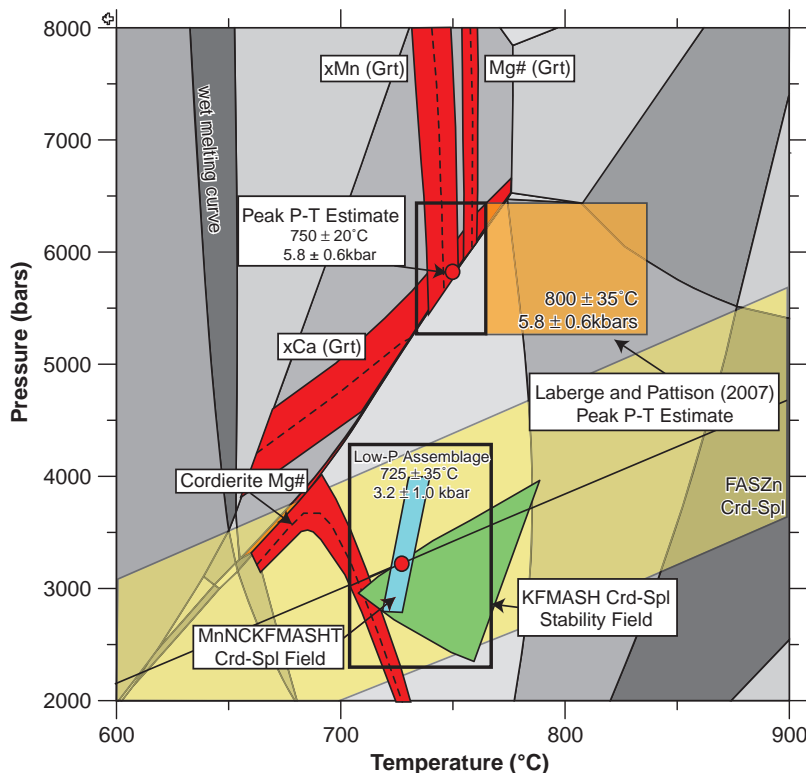


Figure 10. Summary of P-T results from the foot-wall. Garnet mineral isopleth intersections for the sillimanite-garnet-cordierite assemblage suggest a peak P-T of $750 \pm 20^\circ\text{C}$, 5.8 ± 0.6 kbars. This is at an equal pressure but lower temperature than the P-T estimate of Laberge and Pattison (2007). For the decompression assemblage, cordierite mineral isopleths may not accurately represent the decompression assemblage, but lie at a similar pressure to cordierite+spinel stability fields in existing literature (see text for details). A FASZn geobarometry estimate of 3.2 ± 1.0 kbar for coexisting cordierite+spinel in the decompression assemblage passes through the published cordierite+spinel stability fields. Mineral abbreviations as in Figure 5.

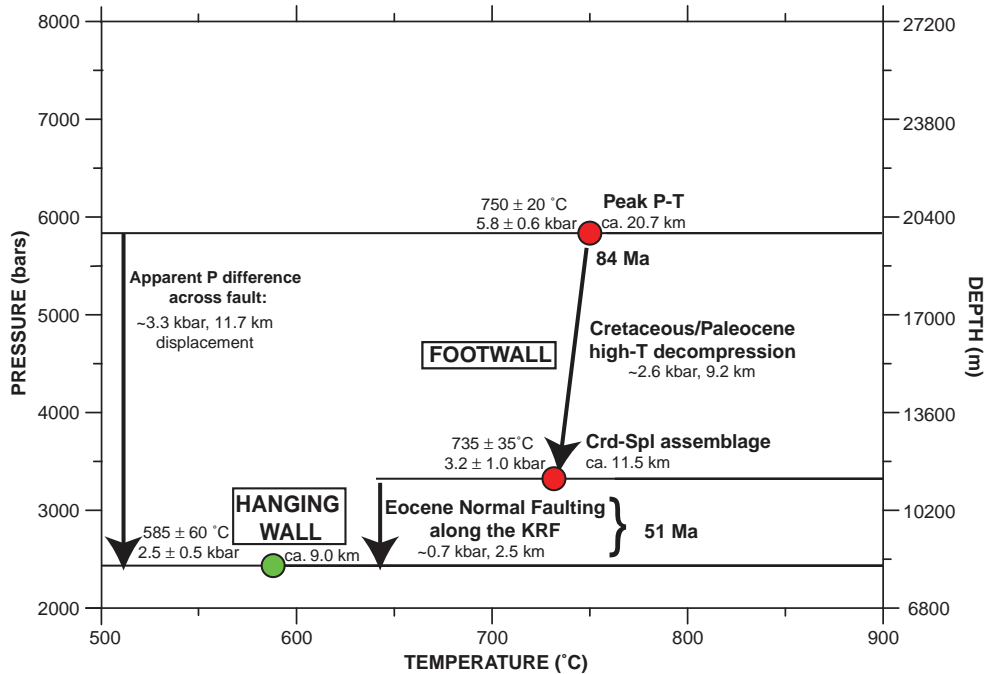


Figure 11. Summary of P-T conditions in the hanging wall and footwall of the Kettle River fault. Pressure-depth conversion assumes $\rho = 2.85 \text{ g/cm}^3$. When Late Cretaceous/Paleocene high-temperature exhumation is taken account, the pressure contrast across the KRF ($\sim 0.7 \text{ kbar}$ or 2.5 km) is much less than that suggested by the metamorphic contrast across the fault ($\sim 3.3 \text{ kbar}$ or 11.7 km). Crd – cordierite, Spl – spinel.

Based on K-Ar geochronology (Stevens et al. 1982; Hunt and Roddick 1990), the western portion of the Grand Forks Complex passed through the closure temperature of hornblende ($\sim 530^\circ\text{C}$) at $60.5 \pm 2.1 \text{ Ma}$, a weighted mean of results from a single locality. This predates movement on the Kettle River fault (at $51\text{--}50 \text{ Ma}$ from Carr and Parkinson, 1989; Pearson and Obradovich, 1977), indicating that a significant high-temperature exhumation event must have occurred before faulting. This high temperature decompression must additionally have occurred after $84 \pm 3 \text{ Ma}$, the date of peak metamorphism in the Grand Forks gneisses on the western edge of the complex (Laberge and Pattison, 2007). Figure 12 shows a temperature-time interpretation for the complex adapted from Laberge and Pattison (2007) that shows the window of possible timing for this early high-temperature exhumation, assuming that peak metamorphism and exhumation occurred at the same time across the complex. Similar high-temperature decompression events in this time period have been proposed for the Monashee Complex by Norlander et al. (2002) and Johnston et al. (2000), and the Valhalla Complex by Gordon et al. (2008).

Recognition of the low-pressure spinel+cordierite+ilmenite assemblage is crucial to constraining the pressure contrast across the Kettle River normal fault. The difference in peak metamorphic pressure between the footwall ($5.8 \pm 0.6 \text{ kbar}$, $20.7 \pm 2 \text{ km}$) and the hanging wall ($2.5 \pm 0.5 \text{ kbar}$, $9.0 \pm 1.7 \text{ km}$) is $\sim 3.2 \text{ kbar}$ (11.7 km), is ostensibly suggestive of a major exhumation event focused along the Kettle River fault (Fig. 11). However, by removing the

effects of the pre-Eocene, high-temperature decompression event, the pressure contrast is reduced to $\sim 0.7 \pm 1.5 \text{ kbar}$ ($\sim 2.5 \pm 5 \text{ km}$). The estimate for the Kettle River fault presented in this study is within error of the estimate of Laberge and Pattison (2007) for displacement along the Granby fault, $5 \pm 3.5 \text{ km}$. It is important to note that barometry in Laberge and Pattison (2007) was conducted upon metasilicites from the Carboniferous-Permian Knob Hill Group (Laberge and Pattison, 2007), which based on lithological distinctions is not correlative with the Pennsylvanian-Permian Mollie Creek assemblage in the Christina Lake area (Acton et al., 2002). In the Greenwood-Grand Forks area, the Knob Hill group is unconformably overlain by the Triassic Brooklyn Formation, as well as rocks of the early Jurassic Rossland Group (Acton et al., 2002). By comparison, in the hanging wall to the KRF, the Mollie Creek assemblage is unconformably overlain by the Elise Formation of the Rossland Group, with no intervening Triassic sedimentary stratigraphy equivalent to the Brooklyn formation. The thickness and extent of the Triassic Josh Creek diorite in the Christina Lake area is unconstrained. Thus, it is possible that the overlying stratigraphic thickness in the hanging wall to the KRF, with a lack of Triassic stratigraphy was significantly less than that in the hanging wall to the Granby fault.

The extent to which this depth contrast measures of the magnitude of Eocene displacement across the KRF depends on a number of assumptions. If metamorphism in the hanging wall and footwall was contemporaneous, and the analyzed rocks that furnished the above P-T estimates

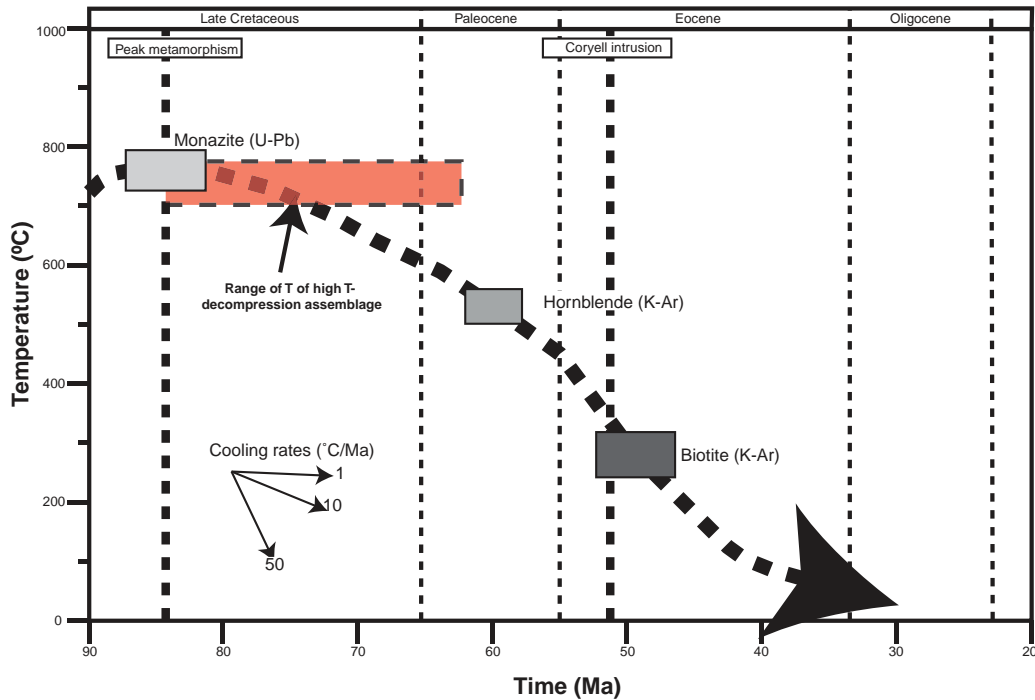


Figure 12. Temperature-time path for the exhumation of the Grand Forks Complex, adapted from Laberge and Pattison (2007). Note that while the exact P-t path is not well constrained between the monazite U-Pb and hornblende K-Ar closure temperatures, the decompression event producing the cordierite-spinel coronas (stable at $725 \pm 35^\circ\text{C}$) must have preceded 60.5 ± 2.1 Ma, and hence movement along the Kettle River fault (51–50 Ma).

were adjacent to the fault with continuous isobaric surfaces immediately prior to faulting, this depth contrast would provide a good estimate of Eocene movement across the KRF. However, the first assumption is known to be incorrect, as footwall metamorphism is estimated to be Cretaceous at 84 ± 3 Ma (Laberge and Pattison, 2007), much later than the mid-Jurassic contact metamorphism that produced the mineral assemblages used for pressure estimation in the hanging wall. If the hanging-wall sedimentary rocks were buried further prior to peak Cretaceous metamorphism in the footwall, the pressure contrast between hanging wall and footwall assemblages would be reduced compared to the above estimate. Alternatively, if significant erosion of the hanging wall occurred between the Middle Jurassic and Late Cretaceous, the hanging wall could have been at a depth less than 9.0 km (2.5 kbar) at the time of footwall Cretaceous peak metamorphism, resulting in a greater fault-related displacement compared to the above estimate.

The fact that Late Jurassic-Early Cretaceous granites of similar composition and texture (unit JKg in Figure 2) intrude both the hanging wall and footwall to the KRF (Höy and Jackaman, 2005) suggests that the hanging wall and footwall could not have been at markedly different crustal levels at the time of Cretaceous metamorphism. In addition, because coarse-grained intrusive rocks of the 51 Ma Coryell Batholith intruded the hanging wall to the Kettle River fault

and sealed its movement north of Christina Lake, the currently exposed hanging-wall lithologies cannot have been very close to the surface at the time of faulting.

In summary, the estimated depth contrast of $\sim 2.5 \pm 5$ km may be a reasonable measure of the displacement across the KRF, within fairly large uncertainties. Laberge and Pattison (2007) provided stratigraphic arguments in support of their estimate of approximately 5 km of displacement across the Granby fault on the west margin of the complex, but whether these arguments pertain to the east side of the complex is uncertain. Regardless, Eocene movement along the Kettle River fault appears to have been a relatively minor last episode in the overall exhumation history of the GFC, accounting for only about 25% of uplift.

ACKNOWLEDGMENTS

J.F. Cubley would like to thank P.O. Hoskin and P.S. Simony for their insights into geochemical and structural interpretation, and E.D. Ghent for assistance in sample petrography. R.G. Anderson and J. Ryan are thanked for their constructive reviews of the manuscript. C. Bettigole, S. Wing and G. Quade are recognized for their aid of fieldwork activities. Research funded by a Geoscience BC scholarship to J.F. Cubley, a contract to J.F. Cubley and D.R.M. Pattison from Targeted Geoscience Initiative 3, Cordilleran Project TG6005, and NSERC Discovery Grant #037233 to D.R.M. Pattison.

REFERENCES

- Acton, S.L., 1998. Geology of the Christina Lake area, B.C.; M.Sc. thesis, University of Calgary, Calgary, Alberta, 110 p.
- Acton, S.L., Simony, P.S., and Heaman, L.M., 2002. Nature of the basement to Quesnel Terrane near Christina Lake, Southeastern British Columbia; *Canadian Journal of Earth Sciences*, v. 39, p. 65–78. doi:10.1139/e01-056
- Armstrong, R.L., 1988. Mesozoic and Early Cenozoic magmatic evolution of the Canadian Cordillera; in *Continental lithospheric deformation*, Geological Society of America, Special Paper 218, p. 55–91.
- Armstrong, R.L., Parrish, R.R., van der Heyden, P., Scott, K., Runkle, D., and Brown, R.L., 1991. Early Proterozoic basement exposures in the southern Canadian Cordillera; core gneiss of Frenchman Cap, Unit I of the Grand Forks Gneiss, and the Vaseaux Formation; *Canadian Journal of Earth Sciences*, v. 28, p. 1169–1201.
- Bowman, E.C., 1950. Stratigraphy and structure of the Orient area, Washington; Ph.D. thesis, Harvard University, Cambridge, Massachusetts, 161 p.
- R. W. Brock. 1903. Kootenay District; Geological Survey of Canada, Annual Report, new series, Vol. XIII (1900), p. 62–84.
- Carr, S.D. and Parkinson, D.L., 1989. Eocene stratigraphy, age of the Coryell Batholith, and extensional faults in the Granby Valley, southern British Columbia; Geological Survey of Canada, Paper 89-1E, p. 79–87.
- Cheney, E.S., 1980. Kettle dome and related structures of north-eastern Washington; Geological Society of America, Memoir 153, p. 463–483.
- Colpron, M., Logan, J.M., and Mortensen, J.K., 2002. U-Pb zircon age constraint for late Neoproterozoic rifting and initiation of the lower Paleozoic passive margin of western Laurentia; *Canadian Journal of Earth Sciences*, v. 39, p. 133–143. doi:10.1139/e01-069
- Daly, R.A., 1912. Geology of the North American Cordillera at the Forty-ninth Parallel; Geological Survey of Canada, Memoir 38, 857 p.
- Dasgupta, S., Ganguly, J., and Neogi, S., 2004. Inverted metamorphic sequence in the Sikkim Himalayas: crystallization history, P-T history and implications; *Journal of Metamorphic Geology*, v. 22, p. 395–412. doi:10.1111/j.1525-1314.2004.00522.x
- de Capitani, C., 1994. Gleichgewichts-Phasendiagramme: Theorie und Software; *Berichte der Deutschen Mineralogischen Gesellschaft, Beiheft zum; European Journal of Mineralogy*, v. 6, p. 48.
- de Capitani, C. and Brown, T.H., 1987. The computation of chemical equilibrium in complex systems containing non-ideal solutions; *Geochimica et Cosmochimica Acta*, v. 51, p. 2639–2652. doi:10.1016/0016-7037(87)90145-1
- Droop, G.T.R. 1987. A general equation for estimating Fe³⁺ concentrations in ferromagnesian silicates and oxides from microprobe analyses, using stoichiometric criteria; *Mineralogical Magazine*, v. 51, p. 431–435.
- Erdmer, P., Thompson, R.I., and Daughtry, K.L., 1999. Pericratonic Paleozoic succession in Vernon and Ashcroft map areas, British Columbia; in *Current Research 1999-A*, Geological Society of Canada, p. 205–213.
- Fyles, J.T., 1990. Geology of the Greenwood-Grand Forks area, British Columbia; British Columbia Ministry of Energy, Mines, and Petroleum Resources, Open File 1990–25, 19 p.
- Gordon, S.M., Whitney, D.L., Teyssier, C., Grove, M., and Dunlap, W.J., 2008. Timescales of migmatization, melt crystallization, and cooling in a Cordilleran gneiss dome: Valhalla complex, southeastern British Columbia; *Tectonics*, v. 27, TC4010, 28 p.
- Holland, T.J.B. and Powell, R., 1998. An internally consistent thermodynamic data set for phases of petrological interest; *Journal of Metamorphic Geology*, v. 16, p. 309–343. doi:10.1111/j.1525-1314.1998.00140.x
- Holtz, T. and Johannes, W., 1994. Maximum and minimum water contents of granitic melts: implications for chemical and physical properties of ascending magmas; *Lithos*, v. 32, p. 149–159.
- Höy, T., 1987. Geology of the Cottonbelt lead-zinc-magnetite layer, carbonatites and alkali rocks in the Mount Grace area, Frenchman Cap dome, southeastern British Columbia; *British Columbia Ministry of Energy and Mines Bulletin*, v. 80, 100 p.
- Höy, T., 2001. Sedex and Broken Hill-type deposits, northern Monashee Mountains, southern British Columbia; *British Columbia Ministry of Energy and Mines, Geological Fieldwork 2000; Paper*, v. 2000–1, p. 85–114.
- Höy, T., and Dunne, P.E. 1997. Early Jurassic Rossland Group, southern British Columbia. Part I - stratigraphy and tectonics; *British Columbia Ministry of Employment and Investment, Mines and Energy Division, Geological Survey Branch, Bulletin 102*.
- Höy, T. and Dunne, K.P.E., 2001. Metallogeny and mineral deposits of the Nelson-Rossland map area; *British Columbia Ministry of Energy and Mines, Bulletin 109*, 196 p.
- Höy, T. and Jackaman, W., 2005. Geology and mineral potential of the Grand Forks Map Sheet (082E/01), southeastern British Columbia; *British Columbia Geological Survey, Geological Fieldwork 2004, Paper 2005–1*, p. 225–230.
- Hunt, P.A. and Roddick, J.C. 1990. A compilation of K-Ar ages; report 19. in *Radiogenic age and isotopic studies, Report 3*; Geological Survey of Canada Paper 89-02, p. 153–190.
- Johnson, T., Brown, M., Gibson, R., and Wing, B., 2004. Spinell-cordierite symplectites replacing andalusite: evidence for melt-assisted diapirism in the Bushveld Complex, South Africa; *Journal of Metamorphic Geology*, v. 22, p. 529–545. doi:10.1111/j.1525-1314.2004.00531.x
- Johnston, D.H., Williams, P.F., Brown, R.L., Crowley, J.L., and Carr, S.D., 2000. Northeastward extrusion and extensional exhumation of crystalline rocks of the Monashee Complex, southeastern Canadian Cordillera; *Journal of Structural Geology*, v. 22, p. 603–625. doi:10.1016/S0191-8141(99)00185-6
- Laberge, J. and Pattison, D.R.M., 2007. Geology of the western margin of the Grand Forks Complex, southern British Columbia: high-grade Cretaceous metamorphism followed by early Tertiary extension on the Granby Fault; *Canadian Journal of Earth Sciences*, v. 44, p. 199–228. doi:10.1139/E06-101

- Little, H.W., 1957. Kettle River, east half, Similkameen, Kootenay and Osoyoos districts, British Columbia; Geological Survey of Canada, Map 6-1957, scale 1:253 440.
- Nichols, G.T., Berry, R.F., and Berry, D.H., 1992. Internally consistent gahnitic spinel-cordierite-garnet equilibria in the FMASHZn system: geothermobarometry and applications; *Contributions to Mineralogy and Petrology*, v. 111, p. 362–377. doi:10.1007/BF00311197
- Norlander, B.H., Whitney, D.L., Teyssier, C., and Vanderhaeghe, O., 2002. Partial melting and decompression of the Thor-Odin dome, Shuswap metamorphic core complex, Canadian Cordillera; *Lithos*, v. 61, p. 103–125. doi:10.1016/S0024-4937(02)00075-0
- Parrish, R.R., Carr, S.D., and Parkinson, D.L., 1988. Eocene extensional tectonics and geochronology of the southern Omineca Belt, British Columbia and Washington; *Tectonics*, v. 7, p. 181–212. doi:10.1029/TC007i002p00181
- Pearson, R.C. and Obradovich, J.D., 1977. Eocene rocks in north-east Washington – radiometric ages and correlation; *United States Geological Survey Bulletin*, v. 1433, 41 p.
- Preto, V.A.G., 1970a. Structure and petrology of the Grand Forks Group, British Columbia; Geological Survey of Canada, Paper 69-22, 80 p.
- Preto, V.A.G., 1970b. Amphibolites from the Grand Forks quadrangle of British Columbia, Canada; *Geological Society of America Bulletin*, v. 81, p. 763–782. doi:10.1130/0016-7606(1970)81[763:AFTGFQ]2.0.CO;2
- Reed, S.J.B., 1996. Electron microprobe analysis and scanning electron microscopy in geology; Cambridge University Press, 206 p.
- Rhodes, B.P. and Cheney, E.S., 1981. Low-angle faulting and the origin of Kettle dome, a metamorphic core complex in northeastern Washington; *Geology*, v. 9, p. 366–369. doi:10.1130/0091-7613(1981)9<366:LFATOO>2.0.CO;2
- Robinson, P., 1991. The eye of the petrographer, the mind of the petrologist; *The American Mineralogist*, v. 76, p. 1781–1810.
- Ross, G.M. and Parrish, R.R., 1991. Detrital zircon geochronology of metasedimentary rocks in the southern Omineca Belt, Canadian Cordillera; *Canadian Journal of Earth Sciences*, v. 28, p. 512–522. doi:10.1139/e91-045
- Spear, F.S., 1993. Metamorphic phase equilibria and pressure-temperature-time paths; *Mineralogical Society of America, Monograph Series*, 799 p.
- Spear, F.S. and Florence, F.P., 1992. Thermobarometry in granulites: pitfalls and new approaches; *Journal of Precambrian Research*, v. 55, p. 209–241. doi:10.1016/0301-9268(92)90025-J
- Spear, F.S. and Parrish, R.R., 1996. Petrology and cooling rates of the Valhalla Complex, British Columbia, Canada; *Journal of Petrology*, v. 37, p. 733–765. doi:10.1093/petrology/37.4.733
- Spear, F.S., Kohn, M.J., and Cheney, J.T., 1999. P-T paths from anatectic pelites; *Contributions to Mineralogy and Petrology*, v. 134, p. 17–32. doi:10.1007/s004100050466
- Stevens, R.D., Delabio, R.N. and Lachance, G.R. 1982. Age determinations and geological studies, K-Ar isotopic ages, Report 15; Geological Survey of Canada, Paper 81-2, 56 p.
- Tempelman-Kluit, D.J., 1989. Geology, Penticton, British Columbia; Geological Survey of Canada, Map 1736A, scale 1:250 000.
- Tinkham, D.K. and Ghent, E.D., 2005. Estimating P-T conditions of garnet growth with isochemical phase diagram sections and the problem of effective bulk composition; *Canadian Mineralogist*, v. 43, p. 35–50. doi:10.2113/gscanmin.43.1.35
- Unterschutz, J.L.E., Creaser, R.A., Erdmer, P., Thompson, R.I., and Daughtry, K.L., 2002. North American margin origin of Quesnel terrane strata in the southern Canadian Cordillera: Inferences from geochemical and Nd isotopic characteristics of Triassic metasedimentary rocks; *Geological Society of America Bulletin*, v. 114, p. 462–475. doi:10.1130/0016-7606(2002)114<0462:NAMOOQ>2.0.CO;2
- White, R.W., Powell, R., and Holland, T.J.B., 2007. Progress relating to calculation of partial melting equilibria for metapelites; *Journal of Metamorphic Geology*, v. 25, p. 511–527. doi:10.1111/j.1525-1314.2007.00711.x

Geological Survey of Canada Project TG6005-x91